INFLUENCE OF SECONDARY FLOW ON MEANDERING OF RIVERS

K.W. Olesen

Laboratory of Fluid Mechanics
Department of Civil Engineering
Delft University of Technology

Report 1 - 82

Contents

List of table and figures

Table:

Figures:

List of symbols

a	coefficient in model for secondary flow
b	coefficient in model for secondary flow inertia
c	coefficient in model for gravitational force on grains
f	$= \frac{g}{C^2}$. Roughness coefficient
g	acceleration due to gravity
h	depth of flow
i	$= \sqrt{-1}$. Imaginary unit
k	wave number in longitudinal direction
k_w	wave number in transverse direction
l	$= k/k_w$. Relative wave number
l_{max}	$= l$ for $\partial\phi_i/\partial l = 0$
m	number of submerged bars in a cross-section
$\max[\phi_i]$	$= \phi_i$ for $\partial\phi_i/\partial l = 0$
t	time coordinate
u	longitudinal flow velocity
v	transverse flow velocity
x	longitudinal coordinate
y	transverse coordinate
z	vertical coordinate and dimensionless perturbation parameter of the bed
z_b	bed level
C	Chézy roughness coefficient
D	determinant. Eq. (3.13)
F	Froude number
F_s	densimetric Froude number
H_{bar}	height of bars
H_{dun}	height of dunes
I	equilibrium bed slope
L_{bar}	length of bars
L_{dunes}	length of dunes
M_1, M_2	coefficients in linearized bed shear stress model
N_1, N_2	coefficients in linearized transport rate model
Q	flow discharge
S	sediment transport rate per unite width
W	width of channel

β	$= S_0/h_0u_0$. Dimensionless sediment transport rate
δ	direction of bed shear stress
ε	$= f/k_w$
θ	dimensionless shear stress. Shield parameter
κ	$\approx$ 0.4 . von Kárman constant
ρ	mass density of fluid
τ_x, τ_y	bed shear stress in x and y direction, respectively
ϕ	complex celerity
ψ	direction of sediment transport
Δ	relative density of sediment
Φ	dynamic friction angle
χ	degree of development of the secondary flow

Subscripts

o (h_0)	refer to zero order solution
i (ϕ_i)	refer to the imaginary part of a complex number
r (ϕ_r)	refer to the real part of a complex number
' (h')	perturbation parameter
* (h^*)	dimensionless parameter. The bulky star is omitted when that does not lead to confusion

Summary

A linear stability analysis of the governing equations for the bed and flow topography in straight alluvial channels is treated. The flow is described by a horizontal two-dimensional model, but secondary flow due to curvature of the streamlines is included. Further more knowledge about secondary flow inertia achieved in recent years is incorporated.

The analysis suggests that secondary flow plays an important role for the development of meander bends in relatively narrow channels.

The results of the stability analysis are compared with some sandflume data. The agreement is unsatisfactory, but the discrepancy can be explained by insufficient knowledge about the secondary flow properties. However, the sandflume data and the results of the stability analysis exhibit the same trends with respect to dependence of width-depth ratio and alluvial roughness, i.e. increasing width-depth ratio as well as increasing roughness coefficient promotes the formation of alternate bars.

1. Introduction

1.1. General

The flow and bed topography in curved alluvial rivers play an important part in several aspects of river engineering, such as navigability, bank protection and river regulation. Engineering problems concerning this topic are mostly so complicated that they must be investigated using physical scale models or numerical models, as the non-linear character of the governing equations in most cases makes an analytical approach impossible. However, the thorough linearization of the equations, in order to make an analytical solution feasible, is justified for a small group of problems. The river morphology problem concerning the formation of alternate bars in straight alluvial channels may belong to this group of problems.

Stability of straight channels can be of great importance: Unforeseen stability problems in for instance a navigation channel can lead to large costs for dredging. Alternate bars can develop into true bends which bring about additional roughness which in turn can cause inundation of low situated areas. Alternate bars in flume experiments may impede the interpretation of the measured data. And many others.

The present linear stability analysis was initiated by instability occurring in a numerical model for the flow and bed topography in curved alluvial rivers. The original aim was to investigate whether these oscillations had a physical cause or whether they were of pure numerical character. The oscillation occurred in the straight reach before the entrance of a bend, and it was therefore thought that a linear stability analysis for a straight channel would serve as a good first approach.

The study is carried out at the Laboratory of Fluid Mechanics at the Delft University of Technology within the framework of the river bend project of the joint hydraulic research programme T.O.W. (Toegepast Onderzoek Waterstaat) in which Rijkswaterstaat (Governmental Water Control and Public Works department) the Delft Hydraulics Laboratory and the Delft University of Technology participate.

1.2. Previous work

The formation of meanders has been studied by many scientists and from several point of views (see Callander, 1978). It is a widely accepted assumption that deformation of the bed is the fundamental cause of meandering and that erosion of the banks follows at a later stage. The bed is considered to be deformed due to unstable response of a small perturbation of the bed. From this approach several scientists have carried out linear stability analysis in order to find the origin and initial wavelength of meandering and braiding in alluvial streams. In the following a brief revue of some important publications within this topic will be given.

The linear stability analysis are carried out by Engelund and Skovgaard, 1973; Parker, 1976 and Fredsøe, 1978. A common basis for these three analysis is that the considered channels are wide in order to be able to neglect any wall effect, that the channels have a rectangular cross-sectional shape and that the banks are non-erodible. In all three analysis the stability of a double periodic and harmonic perturbation of the bed is investigated.

The analysis carried out by Engelund and Skovgaard is remarkable because a three-dimensional flow model is applied. A parabolic distribution of the longitudinal flow velocity in combination with a finite bottom slip velocity is assumed. This non-uniform vertical distribution of velocity provides for secondary current due to flow curvature, which is a significant advantage of this analysis. The flow is considered to be quasi-steady, which is justified with the classical assumption for a bed level model; i.e. disturbances of the flow travel at much higher celerity than disturbances of the bed. Engelund and Skovgaard are using a model for the direction of the sediment transport, which is not only taking the direction of the flow close to the bed into consideration, but also the gravitational force acting on the grains along a sloping bed. The analysis explains why some channels tend to braid, other tend to meander and why a third group remains straight.

Parker (1976) applied a two-dimensional flow model in his analysis, thus secondary flow is not taken into consideration. Parker is using the equations for unsteady flow, and he obtained a complex fourth degree algebraic equation for the amplification factor. Applying assymtotic expansion he found an approximation for the amplification factor; which

is identical to the expression which can be obtained if the derivatives with respect to time in the flow equation are neglected. The analysis yields that all streams are unstable because Parker neglected the gravitational force acting on the grains, which indeed is a very important stabilizing effect.

In the analysis carried out by Fredsøe (1978) the (steady) flow is essentially described by the same two dimensional flow model as Parker used. So also in this analysis secondary flow due to curvature of the streamlines is neglected. The analysis differs from the previous ones by accounting for the gravitational force from the transverse slope of the bed and by dividing the sediment transport into bed load and suspended load, which makes it possible to take account of the phase lag between the bed shear stress and the transport in suspension.

Recently Ikeda, Parker and Sawai (1981) carried out a linear stability analysis for a channel with erodible banks. The analysis yields wave lengths of the same order of magnitude as the more traditional stability analysis for alluvial streams. This supports the assumption that the alternate bars evolute into true bends.
Finally, it should be mentioned that several authors have attempted to explain the formation of alternate bars and meanders from other approaches. For instance,Einstein and Shen (1964) qualitatively explained the formation of alternate bars by secondary flow induced by different shear stress at the side walls or induced by an asymmetrical cross-sectional shape.

1.3. The present investigation

This report concerns a linear stability analysis of the same type as the ones carried out by among others Engelund and Skovgaard (1973), Parker (1976) and Fredsøe (1978), i.e. the stability of a double harmonic perturbation of the bed in a wide rectangular channel with non erodible banks is investigated. As in the analysis by Parker and Fredsøe a two dimensional flow model is employed. The main difference from these two analysis is that the bed shear stress is not parallel to the main flow direction, but the deviation from the main flow direction due to curvature of the streamlines is taken into account; i.e., secondary flow is

considered although a two dimensional flow model is employed. This is a simpler approach than obtaining the secondary flow field directly from the (linearized) three-dimensional equation (see Engelund and Skovgaard). However, the employment of the present approach is more transparant and it has the advantage that it is possible to identify the influences of the flow and sediment transport which is important for the development of alternate bars. Further on, in this analysis knowledge achieved in recent years about the direction of the sediment transport and about inertia of the secondary flow are incorporated.

2. Mathematical modelling

The basic assumption underlying the mathematical model for the flow and bed topography in alluvial channels is that the flow can be considered quasi-steady, i.e. the flow is assumed to adapt much faster to a change in bed level than the bed level change itself. Therefore the computation of the bed level development can be divided into small time steps, during which the bed is kept fixed and the flow field is considered to be steady. The bed level at the following time step can now be computed by means of the equation of continuity for the sediment. This convenient division between flow computation and bed level computation will be maintained in the following.

Most natural alluvial streams have a large width-depth ratio which suggests a two-dimensional description of the flow. This approach has proved to describe the main flow field rather good when main flow inertia and bed friction dominate, except in a narrow region close to the banks where the wall friction has direct influence. However, when the secondary flow has large influence on the main flow distribution, for instance in a rectangular channel with curved alignment, the two-dimensional model fails.

A mathematical model for time dependent change of the bed level in alluvial channels consists in principle of momentum equation for each considered direction for the flow and an equation of continuity for both the sediment and the flow. In the present case of a depth averaged approach there will be four equations, which consequently can relate only four variables. Since there are more variables in this problem additional constitutive relations (for bed shear stress and sediment transport) must be introduced in order to close the system of equation.

In the following first the steady flow will be treated. The complete depth averaged flow equations will be given, whereupon the unperturbed (zero order) solution and the linearized (first order) equation will be derived. Much attention will be paid to the description of the bed shear stress. Final the linearized equation of continuity for the

sediment will be derived, and the direction and amount of sediment transport will be considered.

2.1. Steady flow model

For the mathematical description of the flow a coordinate system is applied which has the x-axis coinciding with the channel axis and positive in the flow direction, the y-axis horizontal and perpendicular to the x-axis and the z-axis vertical upwards. In this coordinate system the depth averaged flow is described by

$$u\frac{\partial u}{\partial x} + v\frac{\partial u}{\partial y} + g\left(\frac{\partial h}{\partial x} + \frac{\partial z_b}{\partial x}\right) + \frac{\tau_x}{\rho h} = 0 \qquad (2.1)$$

$$u\frac{\partial v}{\partial x} + v\frac{\partial v}{\partial y} + g\left(\frac{\partial h}{\partial y} + \frac{\partial z_b}{\partial y}\right) + \frac{\tau_y}{\rho h} = 0 \qquad (2.2)$$

$$\frac{\partial (hu)}{\partial x} + \frac{\partial (hv)}{\partial y} = 0 \qquad (2.3)$$

in which

g	acceleration due to gravity
h	depth of flow
u,v	depth averaged flow velocity in x and y direction, respectively
z_b	(given) bed level
ρ	mass density of fluid
τ_x,τ_y	bed shear stress in x and y direction, respectively.

Equation (2.3) is exact, whereas the longitudinal and transverse momentum equations, eq. (2.1) and eq. (2.2) respectively, hold good under the assumption that vertical accelerations are negligible (hydrostatic pressure), and that depth averaged product terms of the horizontal velocity components equal the product of the depth averaged velocity. This implies that the main flow is unaffected by the horizontal component of the secondary flow. In case of a considerable curvature of the flow and/or a long bend it is a rather rough approach to neglect the convective influence from the secondary flow. However, no general applicable and adequate way to account for this effect in a two dimensional model is

available. Only for the case of mildly sloping banks and bottom a model, which accounts for secondary flow convection, is developed (Kalkwijk & De Vriend, 1980). Nevertheless, the redistribution of the main flow due to the secondary flow is at least as pronounced in rectangular channels as in channels with mildly sloping banks (De Vriend, 1981b).

In the first place knowledge about the unperturbed solution must be obtained. The unperturbed bed level is given by

$$z_b = z_0 - I_0 \cdot x \tag{2.4}$$

in which z_0 is a reference level (at x=0) and I_0 is the equilibrium slope of the bed. Equation (2.4) inserted in eqs.(2.1), (2.2) and (2.3) in combination with impermeable side wall, which provides the boundary conditions, yields the following zero order solution

$$\begin{aligned} h &= h_0 \\ u &= u_0 = \frac{Q}{Wh_0} \\ v &= 0 \\ \tau_x &= \tau_0 = \rho g\, I_0 h_0 \\ \tau_y &= 0 \end{aligned} \tag{2.5}$$

where Q is the total discharge and W the width of the channel.

In order to make the stability analysis feasible the flow model, eqs. (2.1), (2.2) and (2.3), must be linearized. This is done by superimpose a small perturbation to the zero order solution in the form:

$$\begin{aligned} h &= h_0 + h' & h' &\ll h_0 \\ u &= u_0 + u' & u' &\ll u_0 \\ v &= 0 + v' & v' &\ll u_0 \\ z_b &= z_0 - I_0 x + z' & z' &\ll h_0 \\ \tau_x &= \tau_0 + \tau_x' & \tau_x' &\ll \tau_0 \\ \tau_y &= 0 + \tau_y' & \tau_y' &\ll \tau_0 \end{aligned} \tag{2.6}$$

Inserting this perturbed solution into the flow equation (2.1), (2.2) and (2.3) and neglecting second and higher order terms leads to the linearized flow equations

$$u_0 \frac{\partial u'}{\partial x} + g\left(\frac{\partial h'}{\partial x} + \frac{\partial z'}{\partial x}\right) + \frac{\tau_0}{\rho h_0}\left(\frac{\tau_x'}{\tau_0} - \frac{h'}{h_0}\right) = 0 \tag{2.7}$$

$$u_0 \frac{\partial v'}{\partial x} + g\left(\frac{\partial h'}{\partial y} + \frac{\partial z'}{\partial y}\right) + \frac{\tau_0}{\rho h.} \frac{\tau_y'}{\tau_0} = 0 \tag{2.8}$$

$$h_0 \frac{\partial u'}{\partial x} + u_0 \frac{\partial h'}{\partial z} + h_0 \frac{\partial v'}{\partial y} = 0 \tag{2.9}$$

For convenience dimensionless variables will be introduced. For this transformation the depth of flow h_0 will be used as the characteristic length scale and h_0/u_0 as characteristic time scale. For instance $h = h'/h_0$, $z^* = z'/h_0$, $v^* = v'/u_0$ etc. The asterisks indicate dimensionless perturbation variables, but will be omitted when that does not give rise to confusion. The dimensionless set of equations now becomes

$$\frac{\partial u}{\partial x} + F^{-2}\left(\frac{\partial h}{\partial x} + \frac{\partial z}{\partial x}\right) + f(\tau_x - h) = 0 \tag{2.10}$$

$$\frac{\partial v}{\partial x} + F^{-2}\left(\frac{\partial h}{\partial y} + \frac{\partial z}{\partial y}\right) + f\,\tau_y = 0 \tag{2.11}$$

$$\frac{\partial u}{\partial x} + \frac{\partial v}{\partial y} + \frac{\partial h}{\partial x} = 0 \tag{2.12}$$

in which F is the Froude number holding for the unperturbed flow situation

$$F = \frac{u_0}{\sqrt{g\,h_0}} \tag{2.13}$$

and f a roughness coefficient defined as

$$f = \frac{\tau_0}{\rho\, u_0^2} = \frac{g}{C^2} \tag{2.14}$$

in which C is the wellknown Chézy roughness coefficient.

2.2 Bed shear stress

For two reasons the bed shear stress deserves some extra attention. First, the shear stress must be eliminated by a constitutive relation in order to close the system of equations (2.1), (2.2) and (2.3). Second, the direction of the bed shear stress, which generally will deviate from the main flow direction due to secondary flow, has a large influence on the direction of the sediment transport.

The traditional method to express the bed shear stress by means of the flow parameter is Chézy's law, which, for uniform flow, implies that the shear stress is proportional to the square of the mean flow velocity. In a horizontal two-dimensional flow the bed shear stress is often expressed by

$$\tau_x = \rho f u \sqrt{u^2 + v^2}$$
$$\tau_y = \rho f v \sqrt{u^2 + v^2} \qquad (2.15)$$

which holds good in case of no secondary flow. As a first approximation eq. (2.15) is applied in the flow model, i.e. the secondary flow is only taken into account in the model for the sediment movement.

As the roughness coefficient is not a constant, the variation of f must be expressed in terms of the flow parameters. However no general applicable and reliable model is available. Several scientists using different approaches have dealt with roughness prediction, and general agreement seems to exist about a functional relationship for the roughness coefficient like

$$f = f(F_s, I) \qquad (2.16)$$

in which $F_s = \frac{u_0}{\sqrt{g\Delta d}}$ is the densimetric Froude number, Δ is the relative density of the sediment compared to the density of the water and d is a characteristic diameter of the sediment. Thus the bed shear stress actually is a function of the flow velocity and the slope. The constitutive relation can then be linearized by means of a double Taylor serie expansion into these two variables. The terms in eqs. (2.10) and (2.11), which contains the shear stress, can then be approximated by (see also Parker, 1976)

$$f\ (\tau_x - h) = f_0\ (M_1 u - M_2 h) \tag{2.17}$$

$$f\ \tau_y = f_0 v \tag{2.18}$$

in which M_1 and M_2 are given by

$$M_1 = (2 + \frac{u_0}{f_0}\ \frac{\partial f_0}{\partial u_0}) \ /\ (1 - \frac{I}{f_0}\ \frac{\partial f_0}{\partial I})$$

$$M_2 = 1 \ /\ (1 - \frac{I}{f_0}\ \frac{\partial f_0}{\partial I})$$

In case of a constant roughness coefficient $M_1 = 2$ and $M_1 = 1$.

In a curved flow there is a transverse circulation due to the non-uniform vertical distribution of the main flow. For that reason the direction of the flow close to the bottom will deviate from the direction of the depth averaged flow. In case of fully developed flow in a wide curved channel the horizontal component of this secondary flow is often found by solving the momentum equation in transverse direction, disregarding all lateral friction terms and all inertia terms except the centrifugal ones. Applying this procedure the direction of the bed shear stress can be expressed like

$$\tan \delta = - a \frac{h}{R} \tag{2.19}$$

in which δ is the angle between the shear stress and the direction of the channel axis, R is the radius of curvature of the channel and a is a constant depending on the model for the longitudinal flow. Rozowski (1957) found a = 10 $\sim$ 12 for a logarithmic velocity profile. Later De Vriend (1977) modified Rozowski's theory and found $a = 2/\kappa^2\ (1 - \frac{\sqrt{f}}{\kappa})$ in which $\kappa \approx 0{,}4$ is the von Kármán constant. Engelund (1974) obtained a $\approx$ 7 for a parabolic distribution of the longitudinal flow velocity. For a parabolic velocity distribution in the upper part of the flow and a logarithmic in the lower part Knudsen (1981) found a $\approx$ 10 $\sim$ 11. Thus a = 10 is a representative theoretical value.

So far the model for the direction of the bed shear stress is based on pure theoretical considerations for an idealized channel. Experiments in curved flumes with smooth bed and finite width show that the theoretical models tend to underestimate the magnitude of the shear stress angle (Yen, 1965 and De Vriend, 1979). Further more according to the theory

the direction of the flow changes rapidly close to the bed. Therefore, when the bed is covered with bedforms, the choice of a representative level for calculation of the bed shear stress introduces a great deal of uncertainty in the bed shear stress angle.

In a developing flow (e.g. entrance and exit of a bend) the streamline curvature does not equal the channel curvature. However it is assumed that eq. (2.19) also applies for the angle between the streamlines and the bed shear stress in a developing flow. In this case the angle between the bed shear stress and the channel axis becomes

$$\tan \delta = \frac{v}{u} - a \frac{h}{R_s} \tag{2.20}$$

in which R_s is the radius of curvature of the streamline. In a straight channel the streamline curvature can be approximated by (De Vriend, 1978)

$$\frac{1}{R_s} = - \frac{1}{u} \frac{\partial v}{\partial x} \tag{2.21}$$

Combining eq. (2.20) and (2.21) leads to a model for the direction of the bed shear stress in terms of the dependent variables

$$\tan \delta = \frac{v}{u} + a \frac{h}{u} \frac{\partial v}{\partial x} \tag{2.22}$$

This model applies if the secondary flow is considered to respond immediately to a change in flow curvature. As well as the main flow, the secondary flow will need a certain length after the beginning of a bend before it is fully developed, and a certain length to decay beyond a bend. It is very important to have a description of this retarded adaption to change in curvature, because the streamline curvature of the flow over alternate bars rapidly changes sign.

De Vriend (1981) suggested to describe this secondary flow inertia by means of a damped exponential function like

$$\frac{b}{\sqrt{f}} h \frac{\partial \chi}{\partial x} + \chi = \frac{h}{u} \frac{\partial v}{\partial x} \tag{2.23}$$

in which χ is a variable representing the degree of development of the

secondary flow and b is a dimensionless constant. According to De Vriend b ≈ 1.3. The direction of the bed shear stress is now given by

$$\tan \delta = \frac{v}{u} + a \chi \tag{2.24}$$

In appendix A it is outlined how De Vriend obtained this model. The model for the secondary flow inertia is based on considerations about the decay of the helical flow after a bend in a vertical plane through a straight streamline. Further more derivatives in y-direction (except the pressure) are considered much smaller than derivatives in z-direction and consequently they are neglected. This is of course a very schematic approach, and it may not be justified to employ the model to the development of the secondary flow in case of curved streamlines and/or in narrow channels. Further more so far only experimental verification for smooth bed have been carried out (De Vriend, 1981).

The model for the direction of the shear stress and the secondary flow inertia yields, when linearized and made dimensionless in the same way as before

- without secondary flow inertia

$$\tan \delta = v + a \frac{\partial v}{\partial x} \tag{2.25}$$

- with secondary flow inertia

$$\frac{b}{\sqrt{f}} \frac{\partial \chi}{\partial x} + \chi = \frac{\partial v}{\partial x} \tag{2.26}$$

$$\tan \delta = v + a \chi \tag{2.27}$$

in which v, δ and χ are dimensionless perturbation parameters.

2.3. Equation of continuity for the sediment

The mass balance for the sediment yields

$$\frac{\partial z_b}{\partial t} + \frac{\partial s_x}{\partial x} + \frac{\partial s_y}{\partial y} = 0 \tag{2.28}$$

in which s_x and s_y are sediment transports per unit width in x and y direction, respectively. The direction of the sediment transport ψ is defined as

$$\tan \psi = \frac{s_y}{s_x} \tag{2.29}$$

By means of eq. (2.29) the transverse sediment transport in eq. (2.28) can be eliminated. The equation of continuity then becomes

$$\frac{\partial z_b}{\partial t} + \frac{\partial s_x}{\partial x} + \tan \psi \frac{\partial s_x}{\partial y} + s_x \frac{\partial \tan\psi}{\partial y} = 0 \tag{2.30}$$

The zero order solution of eq. (2.30) in combination with the unperturbed flow yields

$$z_b = z_0 - Ix$$

$$s_x = s_0 \tag{2.31}$$

$$\tan \psi = 0$$

Superimposing a slight perturbation to the zero order solution, inserting in eq. (2.30) and neglecting second and higher order terms leads to the linearized equation of continuity

$$\frac{\partial z'}{\partial t} + \frac{\partial s'}{\partial x} + s_0 \frac{\partial \tan\psi'}{\partial y} = 0 \tag{2.32}$$

Dimensionless variables will be introduced as follows:

$$z^* = z'/h_0$$
$$x^* = x/h_0$$
$$y^* = y/h_0$$
$$s^* = s'/s_0$$
$$t^* = t u_0/h_0$$

In terms of these dimensionless perturbation variables the equation of continuity becomes

$$\frac{1}{\beta} \frac{\partial z}{\partial t} + \frac{\partial s}{\partial x} + \frac{\partial \tan\psi}{\partial y} = 0 \tag{2.33}$$

in which the asterisks · have been omitted. β is the ratio between the specific discharges of the flow of the sediment evaluated in the unpertubed situation, i.e. $\beta = \frac{s_0}{u_0 h_0}$.

2.4. Sediment transport

The magnitude and direction of the sediment transport must be expressed in terms of the dependent parameters in order to close the system of equations. In principle the stability analysis is based on eq. (2.33), so a proper description of the sediment transport properties is very important. Therefore this point demands some attention.

A large number of formulae which relate the amount of sediment transport and the flow parameters are available. A good deal of the transport formulae yields that the transport rate is a function of the dimensionless shear stress (Shield parameter) $\theta = hI/\Delta d$ and possibly more parameters, i.e.

$$s = s(\theta, ...) \tag{2.34}$$

By means of a double Taylor serie expansion the perturbed dimensionless sediment transport can be approximated by

$$s = N_1 u - N_2 h \tag{2.35}$$

in which N_1 and N_2 are given by (Parker, 1976)

$$N_1 = \frac{u_0}{s_0}\frac{\partial s_0}{\partial u_0} + \frac{I_0}{s_0}\frac{\partial s_0}{\partial I_0} M_1$$

$$N_2 = \frac{I_0}{s_0}\frac{\partial s_0}{\partial I_0} M_2$$

M_1 and M_2 are defined at p.10. Both N_1 and N_2 and M_1 and M_2 are evaluated in the unpertubed situation.

Models for the direction of the sediment transport are scarce. Three theoretical models will be considered here. The models are based on the assumption that a gravitational force acting along the inclined bed causes a deviation of the direction of transport from the direction of the bed shear stress. The models are

- Engelund (1974) -

$$\tan \psi = \tan \delta - \frac{1}{\tan\Phi} \frac{\partial z}{\partial y} \tag{2.36}$$

- Koch (1980) -

$$\tan \psi = \frac{\sin\delta - \frac{\mu}{\theta} \frac{\partial z}{\partial y}}{\cos\delta - \frac{\mu}{\theta} \frac{\partial z}{\partial x}} \tag{2.37}$$

- Engelund (1981) -

$$\tan \psi = \tan \delta - \frac{0.6}{\sqrt{\theta'}} \frac{\partial z}{\partial y} \tag{2.38}$$

in which Φ is the dynamic friction angle ($\Phi \simeq 30^{o} - 40^{o}$), μ is a factor of the order of magnitude of unity, θ is the Shields parameter and θ' is the effective Shields parameter, i.e. the shear stress related to the skin friction. According to Einstein (1950) θ' can be obtained from

$$\frac{1}{\sqrt{f \frac{\theta'}{\theta}}} = 6 + 2.5 \ln \frac{h_0 \theta'}{2.5d \theta} \tag{2.39}$$

Engelund (1974) used eq. (2.36) to calculate the bed topography in a meandering channel. At first sight the good agreement between theory and experiments supports eq. (2.36). However, if the relevant parameter for the experiments are inserted in eq. (2.37) and eq. (2.38), then the three models are almost identical. Eq. (2.37) is used to calculate the bed profile for a few fully developed bends (Koch, 1980). The agreement between theory and experimental data was satisfactory, but it was necessary to tune the model with the factor μ. Eq. (2.38) is a theoretical model in which a constant (0.6) is determined empirically. The model is tested with a large number of experimental data obtained from three almost 360^{o} bends (data: Zimmermann & Kennedy, 1978). The data confirm the theoretical model but there is a rather large scatter in the data, especially for low Shield parameters. Further more all bends in these experiments had a rather steep transverse slope, and therefore it cannot be taken for granted that the model and/or the empirical constant do apply in case of a weak transverse slope. Consequently the model may not apply in case of a small perturbation. Nevertheless from the three models eq. (2.38) seems most reliable.

With a linearization according to the rules outlined in chapter 2.1 all three models get the form

$$\tan \psi = \tan \delta - c \frac{\partial z}{\partial y} \tag{2.40}$$

in which ψ, δ and z again are dimensionless perturbation parameters. Equation (2.40) will be applied in the following with c calculated according to eqs. (2.38) and (2.39).

3. Solution for a double harmonic perturbation

The stability analysis is in fact an analysis of the development in time of a two-dimensional small amplitude wave superimposed on the equilibrium bed. This perturbation can mathematically be expressed as

$$z = \tilde{z} \begin{bmatrix} \sin(k_w y) \\ \cos(k_w y) \end{bmatrix} \exp i(kx - \phi t) \tag{3.1}$$

in which $\tilde{z}$ is the amplitude of the perturbation, $k_w = m\pi \frac{h_0}{W}$ is the dimensionless wavenumber in transverse direction, m is two times the number of waves in a cross-section, $k = 2\pi\ h_0/L$ the dimensionless wavenumber in longitudinal direction, L the wave length, ϕ the complex celerity and $\sqrt{i} = -1$.

The variables m determine the bed pattern. For m = 1 there is one submerged bar in a cross-section, which corresponds to the early stage of meandering. For m = 2,3 etc. the perturbation of the bed consists of an increasing number of surbmerged bars, which characterizers the incipient braiding river (figure 1).

The solution for the double harmonic perturbation will take place in two steps. First the solution of the flow model will be derived. Next this solution will be used to obtain an expression for the complex celerity; actually being the solution of the equation of continuity.

3.1. Solution of the flow model

The linearized flow model arises from combining the eqs. (2.10),(2.11), (2.12), (2.17) and (2.18)

$$\frac{\partial u}{\partial x} + F^{-2}\left(\frac{\partial h}{\partial x} + \frac{\partial z}{\partial x}\right) + f\ (M_1\ u - M_2 h) = 0 \tag{3.2}$$

$$\frac{\partial v}{\partial x} + F^{-2}\left(\frac{\partial h}{\partial y} + \frac{\partial z}{\partial y}\right) + f\ v = 0 \tag{3.3}$$

$$\frac{\partial u}{\partial x} + \frac{\partial h}{\partial x} + \frac{\partial v}{\partial y} = 0 \tag{3.4}$$

As there is no time dependence in this set of equations, i.e. steady flow, the complex celerity in eq. (3.1) will for the time being be taken equal zero. It is easily seen that the solution has the form

$$z = \tilde{z} \begin{bmatrix} \sin(k_w y) \\ \cos(k_w y) \end{bmatrix} \exp i\, k\, x$$

$$u = \tilde{u} \begin{bmatrix} \sin(k_w y) \\ \cos(k_w y) \end{bmatrix} \exp i\, k\, x \qquad (3.5)$$

$$h = \tilde{h} \begin{bmatrix} \sin(k_w y) \\ \cos(k_w y) \end{bmatrix} \exp i\, k\, x$$

$$v = \tilde{v} \begin{bmatrix} \cos(k_w y) \\ -\sin(k_w y) \end{bmatrix} \exp i\, k\, x$$

in which $\tilde{u}$, $\tilde{h}$ and $\tilde{v}$ are complex amplitudes. The influence of a complex amplitude can be displayed by representing for instance u in polar firm

$$u = r_u \exp i\, \psi_u \begin{bmatrix} \sin(k_w y) \\ \cos(k_w y) \end{bmatrix} \exp i\, k\, x$$

$$= r_u \begin{bmatrix} \sin(k_w y) \\ \cos(k_w y) \end{bmatrix} \exp i\,(kx + \psi_u) \qquad (3.6)$$

in which $r_u = \sqrt{\tilde{u}_r^2 + \tilde{u}_i^2}$ and $\tan \psi_u = \dfrac{\tilde{u}_i}{\tilde{u}_r}$

So the complex amplitude determines the phase and the amplitude of the wave.

Impermeable side walls provide the boundary conditions for the flow model, i.e.

$$v = 0 \quad \text{for } y = \pm \tfrac{1}{2} \frac{W}{h_0} \qquad (3.7)$$

Inserting eq. (3.7) in the solution for v in combination with the definition of k_w yields

$$\tilde{v} \cos\left(\frac{m}{2}\pi\right) \exp i\,k\,x = 0 \quad \Rightarrow m = 1,3,5$$

$$-\tilde{v} \sin\left(\frac{m}{2}\pi\right) \exp i\,k\,x = 0 \Rightarrow m = 2,4,6 \tag{3.8}$$

Consequently the upper solution in eq. (3.6) applies for m odd and the lower one for m even.

The complex amplitude can now be found by solution of a set of simple algebraic equations. Inserting eq. (3.6) into the linearized flow model, eqs. (3.2), (3.3) and (3.4), yields after reduction of the harmonic part

$$i\,k\,\tilde{u} + F^{-2}(i\,k\,\tilde{h} + i\,k\,\tilde{z}) + f\,M_1\,\tilde{u} - f\,M_2\,\tilde{h} = 0 \tag{3.9}$$

$$i\,k\,\tilde{v} + F^{-2}(k_w\,\tilde{h} + k_w\,\tilde{z}) + f\,\tilde{v} = 0 \tag{3.10}$$

$$i\,k\,\tilde{u} + i\,k\,\tilde{h} - k_w\,\tilde{v} = 0 \tag{3.11}$$

After rearranging and division by k_w the three linear equations can be expressed in matrix-form as

$$F^2 \begin{bmatrix} \varepsilon M_1 + i\,1 & -\varepsilon M_2 + i\,F^{-2}1 & 0 \\ 0 & F^{-2} & \varepsilon + i\,1 \\ i\,1 & i\,1 & -1 \end{bmatrix} \begin{bmatrix} \tilde{u} \\ \tilde{h} \\ \tilde{v} \end{bmatrix} = \tilde{z} \begin{bmatrix} -i1 \\ -1 \\ 0 \end{bmatrix} \tag{3.12}$$

in which $1 = k/k_w$ and $\varepsilon = f/k_w$.

The determinant of this complex matrix can be elaborated to

$$D = \varepsilon\left[M_1 + 1^2(1 - F^2(1 + M_1 + M_2))\right]$$

$$+ i\left[1(1 + \varepsilon^2 F^2(M_1 + M_2)) + 1^3(1 - F^2)\right] \tag{3.13}$$

The solution of the three complex variables finally are

$$\tilde{u} = \frac{\tilde{z}}{D}\left[\varepsilon(1^2 - M_2) + i\ 1^3\right] \tag{3.14}$$

$$\tilde{h} = \frac{\tilde{z}}{D}\left[-\varepsilon(1^2 + M_1) - i\ (1 + 1^3)\right] \tag{3.15}$$

$$\tilde{v} = \frac{\tilde{z}}{D}\ i\ 1\ \left[-\varepsilon\ (M_1 + M_2) - i\ 1\right] \tag{3.16}$$

In figure 2 the phase and the amplitude of $\tilde{u}$, $\tilde{h}$ and $\tilde{v}$ are depicted as a function of the relative wavenumber 1 for two different values of ε. In figure 3 the influence of the Froude number is depicted. In both cases the roughness coefficient is considered to be independent of the flow parameters, so $M_1 = 2$, and $M_1 = 1$.

The phase lag of the water depth is almost constant π and the amplitude is close to unity, at least for moderate Froude number and for long waves in longitudinal direction. In this case the rigid-lid approximation applies, i.e.

$$h = - z \tag{3.17}$$

This is a very attractive approximation because a perturbation of the depth of flow can be considered instead of a perturbation of the bed level. Consequently one dependent variable can be eliminated. Reducing $\tilde{z}/D$ from eqs. (3.14), (3.15) and (3.16) yields

$$\tilde{u} = \tilde{h}\ \frac{\varepsilon(M_2 - 1^2) - i\ 1^3}{\varepsilon(M_1 + 1^2) + i(1 + 1^3)} \tag{3.18}$$

$$\tilde{v} = \tilde{h}\ i\ 1\ \frac{\varepsilon(M_1 + M_2) + i\ 1}{\varepsilon(M_1 + 1^2) + i(1 + 1^3)} \tag{3.19}$$

The result is now independent of the Froude number. Note that eqs. (3.18) and (3.19) always apply independent of the rigid-lid approximation.

Figure 2 provides the possibility of making some reflections about the cause of the instability. For a given wave length the phase lag between u and z will be equal to $\frac{\pi}{2}$, which corresponds to maximum positive gradient of u at the same location where z is minimal. A simple one dimensional equation of continuity for the sediment, in which the sediment transport is considered to be proportional to the flow velocity, reads

$$\frac{\partial z}{\partial t} + \left(\frac{\partial s_0}{\partial u_0}\right) \frac{\partial u}{\partial x} = 0 \tag{3.20}$$

In the case considered $\frac{\partial z}{\partial t}$ will be negative and the amplitude of the perturbation will grow. In the present analysis the occurrence of maximum instability is more complicated than outlined here because features like transverse transport, secondary flow e.t.c. are taken into consideration. However, the phase lag between u and z of about $\frac{\pi}{2}$ is still one of the dominant factors.

3.2. The stability analysis

To carry out the stability analysis eq. (3.1) and similar perturbations for u, v and h are introduced into the linearized equations of continuity for the sediment. The real part of the celerity ϕ_r in eq. (3.1) is related to the migration velocity of the perturbation, whereas the imaginery part ϕ_i is the exponential growth rate as

$$z = \tilde{z} \begin{bmatrix} \sin(k_w y) \\ \cos(k_w y) \end{bmatrix} \exp i(kx - \phi t) = \tag{3.21}$$

$$\tilde{z} \exp \phi_i t \begin{bmatrix} \sin(k_w y) \\ \cos(k_w y) \end{bmatrix} \exp i(kx - \phi_r t)$$

For $\phi_i < 0$ the amplitude of the perturbation will decrease, whereas instability occurs for $\phi_i > 0$.

The linearized equation of continuity for the sediment can be expressed in terms of the dependent variables by combining eqs. (2.26), (2.27), (2.33) and (2.40)

$$\frac{1}{\beta} \frac{\partial z}{\partial t} + N_1 \frac{\partial u}{\partial x} - N_2 \frac{\partial h}{\partial x} + \frac{\partial v}{\partial y} + a \frac{\partial \chi}{\partial y} - c \frac{\partial^2 z}{\partial y^2} = 0 \tag{3.22}$$

with χ from

$$\frac{b}{\sqrt{f}} \frac{\partial \chi}{\partial x} + \chi = \frac{\partial v}{\partial x} \tag{3.23}$$

Inserting eq. (3.1) and the similar one for the remaining dependent variables and reducing the harmonic part leads to the dispersion equation, which reads

$$\frac{1}{\beta} i \phi \tilde{z} = N_1 i k \tilde{u} - N_2 i k \tilde{h} - k_w \tilde{v} - \frac{a i k}{i k \frac{b}{\sqrt{f}} + 1} k_w \tilde{v} + c k_w^2 \tilde{z} \qquad (3.24)$$

as $\chi = (i k \frac{b}{\sqrt{f}} + 1)^{-1} \frac{\partial v}{\partial x}$

Substituting eqs. (3.14), (3.15) and (3.16) into the dispersion equation gives, after a few manipulations, an expression for the complex celerity

$$\frac{\phi}{\beta} = - i c k_w^2 + \frac{k_w 1}{D} \left[\varepsilon(1^2(N_1+N_2) + N_2M_1 - N_1M_2 + M_1 * M_2 \right.$$

$$\left. + i (1^3(N_1+N_2) + 1(N_2+1)\right] \qquad (3.25)$$

$$+ a \frac{k_w^2}{D} (i \frac{b1}{\sqrt{f}} k_w + 1)^{-1} \left[- 1^3 + i \varepsilon 1^2(M_1+M_2)\right]$$

In which D is given by eq. (3.13)

The three main terms in eq.(3.25)can be attributed to different effects. The term "$- i c k_w^2$ " is due to the gravitational force on the grains along the transverse slope of the bed. The term "k_w 1/D [...] " describes the influence of the main flow on the complex celerity. This term is identical with the expression Parker (1976) based his stability analysis on. The remaining term is new in this type of analysis. It accounts for the influence of the secondary flow on the stability of the bed.

The expression for the complex celerity is not very transparant. A short sensitivity analysis will be carried out in order to illustrate the influence of the different variables and parameters. However, first a discussion of the basic assumptions, which underlies this analysis, will be presented.

4. Discussion on basic assumption

Always when dealing with sediment transport in alluvial channels a great deal of uncertainty in the prediction of the transport rate and the alluvial roughness is present. Of course this also applies to this analysis of the linearized equations. However, in the present case of a two-dimensional approach, the major source of uncertainty originates from the model for the direction of the bed shear stress (secondary flow) and from the model for the direction of the sediment transport. In chapter 2 the reliability of the models for the secondary flow and for the transport direction were briefly treated. A thorough discussion of the roughness and transport rate prediction is out of the scope of this report. In the following a brief discussion of the problems which are specific for the present approach will be given.

A condition for the validity of the approach is that the considered submerged bars differ significantly from the bed forms. For instance if the length of the alternate bars and the dunes are of the same order of magnitude, then the amplitude of the alternate bars must be much larger than the dune height in order to avoid any appreciable influence on the flow(phase lag etc.). The other way around, if the amplitude of the alternate bars is of the same order of magnitude as the dune height, then their length must be much larger than the length of the dunes in order to enable an averaging procedure over the large scale bedform.

The height of the dunes is typical 10% - 20% of the depth of flow, so the height of the alternate bars will always be of the same order of magnitude, for instance never a factor 10 larger. Therefore this analysis applies to the cases where the alternate bars are much longer than the dunes. Several investigators have related the dune length to the depth of flow. Yalin (1964) suggested the dune length - depth of flow ratio to equal five. This analysis indicates a length of the alternate bars which is of the order of magnitude of three times the width. An expression for the dune length - alternate bar length ratio then becomes

$$L_{dunes} \; / \; L_{bars} = \frac{5}{3} \frac{h_0}{W} \qquad (4.1)$$

Consequently this analysis only applies to channels with small depth-width ratios.

Another questionable point in this analysis is the linearization of the model. Below, first a discussion on the linearization of the flow model will be given, next the linearization of the bed level model will be treated

4.1. Linearization of the flow model

The flow model is known to be only weakly non-linear. A suitable way to demonstrate this is to compare the solution of the linearized flow model with the solution obtained by a computational model, which also takes the non-linear terms into consideration.

In figure 4 the result of such a comparison is depicted. The non-linear result is obtained with a computational flow model which disregards the transverse friction (Olesen, 1982). The linear solution, according to eqs. (3.18) and (3.19), are corrected for this omission.

It is expected that a short wave in longitudinal direction will course the largest difference between the two models. In figure 4 the wave length in longitudinal direction is two times the width (l=1) and the amplitude $\tilde{h}$=0.10 which corresponds to the order of magnitude of the dune height. Even in this case the linearization does not give rise to any appreciable discrepancy. Thus the linearization of the flow model does not contest the validity of this stability analysis.

4.2. Linearization of the sediment model

The sediment transport model has a strongly non-linear character, which first of all originates from the non-linear dependence of the transport rate on the flow velocity. The non-linear character causes a deformation of an initial sinuscoidal wave and finally a shock will be formed. The deformed wave can very well be described by a Fourier serie. Unfortunately the application of a Fourier serie would impede the analysis considerable. The analysis would lead to a complex celerity which would depend on the longitudinal coordinate x, i.e. the wave would deform and the initial Fourier serie would no longer apply.

However, in case of a small amplitude of the perturbation non-linear effect is negligible. The linear approach may therefore at least give a satisfactory initial growth or damping rate. Thus the linearization does not so much effect the ability of this analysis to distinguish between stable and unstable

rivers, whereas the propagation and damping/amplification of a perturbation with a certain amplitude may be treated somewhat incorrectly due to non-linear effect.

5. The complex celerity

As mentioned before the real part of the complex celerity gives information about the migration velocity of the perturbations and the imaginary part shows the rate of growth. The imaginary part of the celerity can therefore be used to distinguish between stable and unstable rivers as a positive ϕ_i corresponds to increasing amplitude of the disturbance and a negative one corresponds to a decreasing amplitude.

The analysis also yields the prevailing wave length. In figure 5 the amplification factor (the imaginary part of the complex celerity) is depicted as a function of l. The usual assumption is that alternate bars, with the wave length for which ϕ_i has its maximum, will develop in the stream. This is an obvious assumption, but it can be doubted whether this is the only criterion for the final wave length of the alternate bars. A possibility is that non-linear effect may shift the maximum amplification from one wave length to another, when the amplitude of the perturbation increases. The initial disturbance, which may be related to the bed forms, may have influence on the developing alternate bar pattern. However, as no model exists which accounts for these effects, the present analysis will be based on the assumption that the maximum of ϕ_i determines the wave length of the developing submerged bars.

The complex propagation factor eq. (3.25) is an intricate function of a large number of variables. Therefore it is difficult to recognize, which effect the different variables and terms have on the behaviour of eq.(3.25). Nevertheless the expression for the complex celerity gives already rise to an important observation. The term accounting for the gravitational force is always complex and negative (independend of l), thus it is stabilizing. The magnitude is proportional to the square of k_w, whereas the term accounting for the main flow is proportional to k_w. The secondary flow term increases linearly with k_w for large l and quadraticly for small l. All effects considered there is a large stabilizing effect for large k_w. This corresponds with the observation that narrow channels remain stable.

Regarding the intricacy of the expression for the celerity a sensitivity analysis seems adequate to gain further insight into the behaviour of eq. (3.25).

For this aim it is convenient to divide the variables into three groups.

1. Variables from linearized constitutive relations -
   M_1, M_2, N_1, N_2, a, b and c
2. Variables describing the undisturbed flow situation -
   F, f, β and W ($k_w = m \pi \frac{h}{W}$)
3. Wave number of disturbances -
   k and m ($k_w = m \pi \frac{h_0}{W}$)

The sensitivity analysis will have one example as a point of reference. The undisturbed equilibrium situation for this reference example is given by

$F = 0.25$

$f = 0.01$

$k_w = 0.10$ ($W = 10 \cdot \pi \cdot h_0$ in case of incipient meandering).

The variables from the constitutive relations are assumed to be given by

$a = 10$ (Rozowski, 1957; M. Knudsen, 1981; and many others)

$b = 1.3$ (De Vriend, 1981a)

$c = 1.76$ (Engelund, 1981)

$M_1 = 2.06$ (According to Engelung-Hansen, 1967.
$M_2 = 1.29$ For the elaboration of M_1 and M_2
$N_1 = 5.09$ see Parker, 1976)
$N_2 = 0.43$

$\frac{d}{h_0} = 0.001$ is used for the elaboration of c, M_1,.. N_2. In figure 5 the amplification factor for the reference example is depicted as a function of 1. Here the contribution from the three main terms in eq. (3.25) is also indicated.

In the sensitivity analysis below the influence of one variable at the time will be displayed, so no test for mutual interaction between the variables will be carried out. First the influence of the variables from the constitutive relations and second the variables describing the equilibrium situation will be treated.

5.1. Influence of constitutive relations

The constitutive relations are probably the main source of uncertainty in this analysis. It therefore seems appropriate to gain some insight into this point, before a discussion of the influence of the physical parameters on the development of submerged bars takes place. To this end a short sensitivity analysis is carried out.

The influence of the secondary flow, i.e. the parameters a and b, is illustrated in figure 6 and 7. The magnitude of the secondary current in case of fully developed flow (the parameter a) seems to have only little influence on the wave length, for which the maximum ϕ_i occurs, whereas the influence on the maximum itself seems considerable. The effect of the secondary flow inertia (b) is very significant, and it extends to both the magnitude of the amplification factor and to the wave length l_{max}, for which max $[\phi_i]$ occurs.

Equation (3.25) shows that the term accounting for the gravitational force is independend of l, and that it equals the amplification factor for $l = 0$. Therefore a change of c exclusively effects the magnitude of ϕ, as it only causes a vertical displacement of the graph (see figure 5).

The parameters originate from the linearization of the shear stress model (M_1 and M_2) hardly influence the magnitude of the term accounting for secondary flow, but the effect on the main flow term is rather significant. M_1 (figure 8) has first of all a considerable influence on the 'maximum' wave number l_{max}, whereas the effect on the amplification factor itself is relatively modest. As suggested by figure 9 the contrary applies to M_2.

In figure 10 and 11 the effect of the variables from the linearized model for the sediment transport rate are illustrated. The term in eq. (3.25) which accounts for secondary flow is completely independend of the parameters N_1 and N_2, therefore only the total amplification factors are depicted. The magnitude of max $[\phi_i]$ is strongly effected by change in N_1 where - as l_{max} is almost indifferent. Figure 11 displays that ϕ_i is almost uneffected by a change in N_2. Eq. (3.24) in combination with the fact that the rigid-lid approximation does apply offers an explanation of this. Inserting $\tilde{a} = -\tilde{z}$ in eq. (3.24) shows that N_2 only has influence on the real part of the celerity.

So far there is an inconsistency in the analysis. As mentioned in chapter 2.1., there is not accounted for secondary flow or secondary flow inertia in the flow model but only in the bed level model. In figure 12 the influence of this inconsistency is investigated. The amplification factor is depicted for the bed shear stress parallel to the main flow and parallel to the channel axis. Further on ϕ_i is depicted in case of fully developed secondary flow and in case of secondary flow inertia. The figure shows that a relatively large error is made if the transverse friction is neglected, but it also shows that it is permissible to neglect secondary flow in the flow model (but not in the bed level model), i.e. the inconsistency in this analysis has no appreciable effect.

The sensitivity analysis has not been profound, as there was no test for possible mutual interaction and because only one set of physical parameters was employed. However, it is assumed, that this sensitivity analysis has revealed some general trends. Summarized the conclusions are -

The amplification factor is rather sensitive to the model for secondary flow and especially for the model for secondary flow inertia. The variable c, which accounts for the gravitational force on the grains, has a significant influence on the magnitude of ϕ_i. Further on the linearized model for the alluvial roughness has a noticeable influence on the main flow term. However, the main flow term is most sensitive to the variable N_1, which originates from the linearization of the sediment transport rate with respect to the longitudinal flow velocity. Finally for moderate Froude number the amplification factor is independent of N_2.

5.2. Influence of the flow parameters

An engineer, who for instance has to design a navigation channel, will be very interested in ways to decrease the amplification factor. The engineer hardly has means to influence the parameters discussed above, but he may have the possibility to draw up a design, which insures stability. For this aim the influence of the parameters which describe the undisturbed flow situation and the geometry of the river will be investigated.

The parameters dealt with here are the Froude number (F), the roughness coefficient (f), the ratio between the sediment and water discharge (β) and

the wave number in transverse direction (k_w). The amplification factor is proportional to the parameter β, i.e. β is only related to the rate of growth/decrease of a perturbation. In this analysis β is used as a normalization factor for the complex celerity.

In figure 13 the Froude number is depicted against the maximum value of the imaginary part of the complex celerity max $[\phi_i]$ and against the corresponding wave number l_{max}. If the rigid-lid approximation eq. (3.17) is accepted, the complex celerity is independent of the Froude number (see eqs. (3.18) and (3.19)). The figure confirms that this approximation only applies in case of small Froude number. The influence of moderate Froude numbers on l_{max} is rather significant, whereas the effect on max $[\phi_i]$ is negligible.

The maximum amplification factor as well as l_{max} are increasing approximately linear with the roughness coefficient (figure 14). Although it does not appear very clearly on the graph for max $[\phi_i]$, the variation of l_{max} shows that the influence of the roughness coefficient extends to both the main flow term and to the secondary flow term in eq. (3.25). The trend outlined in figure 14 is in agreement with the assumption that a phase lag on about $\frac{\pi}{2}$ between the bed level and the longitudinal flow velocity is one of the dominant causes of the instability (anyway concerning the main flow). An increased roughness coefficient causes a larger amplitude of the disturbance in the flow velocity and it causes the phase lag of $\frac{\pi}{2}$ to occur for a larger wave number (see figure 2 and recall $\varepsilon = f/k_w$).

The influence from the width of the channel is very significant. In figure 15 the maximum amplification factor is depicted against the transverse wave number. This figure offers an explanation of the fact that some channels tend to braid, other will form meander bends and other remain straight. The wave number k_w^*, for which the ordinate has the same ordinate as the abscissa $2\,k_w^*$, distinguishes between braiding and meandering channels. If $\pi\, h_0/W$ ($= k_w$ for $m = 1$) is smaller than k_w^* then the amplification is larger for $2\,\pi\, h_0/W$ ($= k_w$ for $m = 2$) thus the channel tends to braid. For still wider channels the maximum amplification will occur for still larger m (Engelund & Skovgaard, 1973). It is evident that when the maximum amplification factor is negative the channel will remain straight.

Also the wave number in longitudinal direction for which maximum amplification occurs k_{max} is depicted in figure 15. The dashed line indicates waves which will be damped or will not occur. The full drawn line is almost straight, which implies that the relative wave length 1_{max} is independent of k_w.

In figure 16 a curve similar to figure 15 is depicted, but here the secondary flow is neglected. Comparing the two figures it is noticed, that secondary flow does not play an important role for small wave numbers, whereas the influence is very significant for large k_w. This implies that the secondary flow has a very dominant influence on the stability criterion, whereas the braiding criterion is rather uneffected by the secondary flow.

The secondary flow inertia is essential for this analysis. In figure 17 the secondary flow inertia is neglected (b = 0). Note that the vertical scale is different from the ones in figure 15 and 16. For k_w larger than a particular value there is no longer any maximum but ϕ_i has a horizontal tangent for 1 infinitely great. The absence of a maximum at the curve for max $[\phi_i]$ implies that the river will braid into an infinite number of submerged bars. In figure 18 the gravitational force on the grain is omitted (c = 0). Also in this case the stream will develop an infinite number of submerged bars.

From the point of view of an engineer the stability criterion is of most interest in this analysis. This criterion is very sensitive to the secondary flow and especially to the secondary flow inertia. Unfortunately that is the most unreliable element in this analysis. The shortcomings of the analysis can be emphasized. In case of a wide channel the secondary flow properties are probably relatively good determined, but the main flow term in eq. (3.25) will be predominant. Further more in that case the ϕ_i will be so obvious positive, because also the term accounting for the gravitational force will be rather small, as this term is proportional to k_w^2. The opposite argumentation applies in case of narrow channels. Almost only the gravitational term (stabilizing) and the secondary flow term (destabilizing) contribute to ϕ_i. Further more the magnitude of the two terms is often of the same order of magnitude. In this case it is therefore very important to have an accurate estimate of the secondary flow properties, but in a narrow channel the estimate is encumbered with a large uncertainty.

The analysis cannot be used directly for design purpose before much more knowledge is obtained about the magnitude, the growth and the decay of secondary flow. However for design of stable channels a few trends can be extracted from the analysis so far. First of all it is important to make the channel as narrow as possible. Secondly a small roughness coefficient must be aimed. This can be done for instance by designing for a high bed shear stress so that the bed will not be covered by dunes. A low shear stress (ripple covered bed) will also lead to a small roughness coefficient but in that case the sediment will be close to the point of incipient motion, so N_1 will be large, which increases the amplification factor.

6. Comparison with flume experiments

Regarding the large sensitivity to the secondary flow it is desirable to have measurements of the secondary flow properties for a verification of the model. However measurement of the secondary flow properties in a channel with alternate bars is hardly feasible. Therefore the result of the analysis will be compared to some flume experiments, in which only the main flow properties and the dimension of the alternate bars are measured.

The flume experiments were carried out at the Delft Hydraulics Laboratory De Voorst branche where also the processing of the measured data took place. All data are reported in Wang & Klaassen, 1981. In table 1 the necessary data for the comparison are summarized. The data concerning the bar dimensions depend slightly on the applied filtre technique (strictly speaking the cut-off wave length, see Wang, 1981 and Wang & Klaassen, 1981). The experiments were carried out with a rather uniform sand with a mean diameter of 0,75 mm. The experiment T 34 did not exhibit any instability and for T 26 it is doubtful whether any bars were developed, whereas the remaining experiments exhibited significant alternate bar patterns.

Based on the given data it is in principle possible to design a model for the sediment transport rate and for the bed shear stress for the particular sand, although 9 experiments are rather few to set up these models. In figure 19 the square of the densimetric Froude number ($F_s = u/\sqrt{g\Delta d}$) is depicted against the Shield parameter ($\theta = hI/\Delta d$) for the experiments. According to Chézy's law the line through a particular point and origion will have f^{-1} as slope. A group of experiments is situated at the same line and therefore they have the same roughness coefficient. Two of the tests which are not on this line (T 31 and T 34) are carried out in a flume with another width. The experiment T 19 has an extreme high Froude number and T 14 a very low shear stress, thus other bed form types can be expected in these two experiments. This implies that the roughness coefficient in the flume with the width of 1.50 m is independent of the flow parameter for flows with not too large Froude numbers and not too low bed shear stress. This is very convenient for the calculation of the coefficients from the linearized bed shear stress model, as simply $M_1 = 2$ and $M_2 = 1$.

The sediment transport in kilo per hour per unite width is depicted on double logarithmic paper against the Shield parameter in figure 20. All the experiments, except T 19 which has a very low Froude number, are situated close to a line with a slope of 1.40. As the roughness coefficient is constant this implies that $N_1 = 2.80$ (2 x 1.40) and $N_2 = 0$ for the experiments T 04, T 12, T 23, T 24 and T 26.

As a first approach it is again assumed that

$a = 10$

$b = 1.3$

$c = \frac{0.6}{\sqrt{\theta'}}$,

in which θ' is obtained from the boundary layer equation (2.40).

The amplification factors for the five experiments are depicted against the relatively wave number in figure 21. It appears that the analysis yields that all five flume experiments are stable, whereas the measurements showed that T 04, T 12, T 23 and T 24 were clearly unstable and T 26 may be unstable. This discrepancy may be caused by a wrong choice of a, b and/or c, or this analysis must be rejected as the adequate explanation of the formation of alternate bars.

As mentioned in chapter 2, measurements in curved rectangular flumes show that the theoretical model (a = 10) tends to underestimate the magnitude of the secondary flow. The underestimation can easily amount to a factor two. Furthermore the model for the secondary flow inertia is based on rather schematized theoretical considerations and it is hardly verified. Consequently a large scatter in the coefficient b cannot be rejected. Last but not least the model for the gravitational force is only verified in case of a substantial transverse slope and not in case of a weak slope and the verification of the model showed that a large scatter can be expected. However there is no evidence that this should lead to a systematical underestimation of c and therefore c will be kept unchanged in the following.

A combination of a and b, which cannot be rejected as unrealistic, can be chosen so that the amplification factor becomes positive and maximum for wave numbers which correspond to the experimental findings. In figure 22 a = 25 for all experiments and b = 1.30 for T 04, b = 1.25 (T 12), b = 0.65 (T 23) and b = 0.45 (T 24). The analysis now yields instability and maximum

amplification for the correct wave number, and the choice of a and b is not unrealistic. Consequently the analysis cannot be rejected.

A direct verification of the model is thus not feasible before much more information about the secondary flow properties is obtained. Fortunately it is possible to recognize some trends in the measured data, which correspond well with theoretical findings.

The most important parameter is the transverse wave number, which in the experiments is proportional to the depth width ratio as m = 1. According to figure 15 the maximum amplification factor increases for decreasing k_w, except in a narrow region between the maximum and the wave number k_w^*, which distinguishes between braiding and meandering streams. The same trend is found in the measured data, if it is assumed that increasing dimensionless height of the bars correspond to increasing magnitude of the maximum amplification factor (figure 23).

Also the influence of the roughness coefficient can be investigated. The experiments T 04, T 12, T 14 and T 19 as well as T 23 and T 31 are suitable for this purpose because they have approximately the same depth width ratio ($k_w \approx 0.2$ and $k_w \approx 0.4$, respectively). In figure 24 the measured height and length of the bars are depicted against the roughness coefficient. This figure displays the same trend as suggested by figure 14, i.e. the maximum amplification factor as well as the corresponding wave number l_{max} increase for increasing roughness coefficient.

The Froude number of the experiments is, except T 19, located in a narrow range. Unfortunately there is no suitable experiment to compare T 19 regarding roughness coefficient and depth width ratio.

The experiments do not confirm the validity of the approach, but on the other hand it is not possible to reject the model as an adequate explanation for the information of alternate bars. Similar trends are found in experiment and theory, which supports the validity of the approach.

7. Conclusions and Further research

This report concerns a linear stability analysis of the governing equations for the bed and flow topography in a straight alluvial channel with non-erodible banks. The aim of the analysis was to find the cause and characteristic length scale of incipient meander and braid in rivers. An investigation of the sensitivity to the assumed models for the sediment transport rate, for the bed shear stress and for the secondary flow as well as the sensitivity to the width of the channel, the roughness coefficient and to the Froude number is carried out.

The investigation is an extension of previous work carried out by among others Fredsøe (1978) and Parker (1976), as secondary flow due to flow curvature is taken into consideration. Furthermore a model which accounts for the secondary flow's retarded adaption to change in curvature (secondary flow inertia) is included in the analysis.

The analysis confirms the concept that stability is closely related to the depth width ratio of a stream, i.e. wide channels tend to braid, narrow channels remain straight and in between the channels will form meanders. The analysis also suggests that a high roughness promotes the formation of alternate bars, whereas a high Froude number tends to counteract this. Further more the analysis shows that the sensitivity to various parameters may be of decisive importance for the result of the analaysis.

The trends, which are summarized above, are not different from the results, which would be obtained by an analysis, which did not account for secondary flow. The main influence of the term accounting for secondary flow is that it provides additional instability for first of all short waves in transverse direction. Therefore the secondary flow has not much influence on the formation of braids, whereas the secondary flow may be decisive for whether a channel will remain stable or develop alternate bars.

The performance of the model was compared to some experimental results. The measured data exhibited the same trends as the analysis with respect to depth width ratio and alluvial roughness, which of course supports the

theory. However, an attempt to verify the theory by means of five flume experiments had as a result, that the analysis classified all five experiments as stable, although significant alternate bars were observed in four of the experiments. This discrepancy can be explained by an inaccurate description of the secondary flow, but at the same time it can not be excluded that a dominant additional effect exists. For instance all kind of wall effects have been neglected in this analysis. The effect may extend to a considerable part of the cross-section as the depth width ratio was relatively large. Secondary flow convection, which has proved to have a large influence in rectangular channel bends (De Vriend, 1981b), may also have some influence on the flow over alternate bars, although the curved flow is rather short and the curvature small. Furthermore a necessary condition for the neglect of the effect from the bed form is that the height of the dunes must be much smaller than the height of the alternate bars or; if this condition is not satisfied the wave length of the bars must be much larger than the dune length (Chapter 4). For instance for one of the experiments (T 23) the two relevant ratios are 1.2 (H_{bar}/H_{dun}) and 4.4 (L_{bar}/L_{dun}) (Wang & Klaassen, 1981), thus none of the conditions are satisfied.

For design purpose of e.g. a navigation channel the stability criterion is very important. Unfortunately this criterion is very sensitive to the model for the magnitude of the secondary flow and especially sensitive to the model for the secondary flow inertia, which are the two most unreliable models in this analysis. In case of a rather narrow channel the secondary flow properties are very poorly determined, but the influence of the term is dominant. In a wide channel the secondary flow is better determined but the influence is negligible. Consequently the analysis is not yet suitable for design purpose.

Non-linear effects will probably have some influence on the propagation and growth of the alternate bars when the amplitude becomes finite. To which extend the linearization of the equations contest the validity of the result can be tested, as (non-linear) computational models for the development of the bed and flow topography in alluvial channels already exist (see Koch & Flokstra, 1981).

The performance of the theory can only be improved considerably by improving the description of the secondary flow in relatively narrow channels. That will probably require an accurate description of the flow close to the walls, i.e. also vertical velocity components must be considered. A three-dimensional description of the flow is therefore necessary. With a good model for the eddy viscosity this approach has many advantages compared to the two-dimensional description of the flow. However the computational effort will increase considerably and electronic computers will be necessary even to obtain the zero order solution.

It would also be of great value to extend the analysis to account also for the influence of the bed forms, as the dimensions of the dunes often will be of the same order of magnitude as the dimensions of the submerged bars. The flow over a dune is often computed with a boundary layer model, thus the extension will prohibit a depth averaged description of the flow.

Consequently, a change, which would thoroughly improve the ability to predict whether a channel will remain stable or not, will demand an enormeous computational effort. A time dependent three-dimensional model must be solved, which for the time being is out of the range of most electronic computers.

References

1. Callander, R.A. 1978
River meandering.
Ann. Rev. Fluid Mech. 10, pp. 129-58

2. Einstein, H.A. 1950
The bed-load function for sediment transport in open channel flows.
V.S. Dept. Agric. Tech. Bull. no. 1026

3. Einstein, H.A. & Shen, H.W. 1964
A study of meandering in straight alluvial channels.
J. Geophys. Res. 69, pp. 5239-47

4. Engelund, F. 1974
Flow and bed topography in channel bends.
J. Hydr. Div., Proc. ASCE, vol. 100, no. HY11, pp. 1631-48

5. Engelund, F. 1981
The motion of sediment particles on an inclined bed.
Prog. Rep. 53, pp. 15-20, April, Inst. Hydrodyn. and Hydraul. Engrg.,
Tech. Univ. Denmark

6. Engelund, F. & Hansen, E. 1967
A monograph on sediment transport in alluvial streams.
Copenhagen, Danish Technical Press

7. Engelund, F. & Skovgaard, O. 1973
On the origin of meandering and braiding in alluvial streams.
J. Fluid Mech., vol. 57, part 2, pp. 289-302

8. Fredsøe, J. 1978
Meandering and braiding of rivers.
J. Fluid Mech. vol. 84, part 4, pp. 609-24

9. Ikeda, S., Parker, G. & Sawai, K. 1981
Bend theory of river meanders. Part 1. Linear development.
J. Fluid Mech., vol. 112, pp. 363-77

10. Kalkwijk, J.P.Th., & Vriend, H.J. de. 1980
Computation of the flow in shallow river bends.
J. Hydraul. Res. 18, no. 4, pp. 327-42

11. Koch, F.G. 1980
Bed level computations for axisymmetric curved channels.
Delft Hydraul. Lab. TOW-rep. R657-9/W308, Part I, March

12. Koch, F.G. & Flokstra, C. 1981
Bed level computations for curved alluvial channels.
Proc. 19th IAHR-Congress. New Delhi, India, February.
Also: Delft Hydraul. Lab., Publ. no. 240, Nov. 1980

13. Knudsen, M. 1981
On the direction of the bed shear stress in channel bends.
Prog. Rep. 53, pp. 3-7, April, Inst. Hydrodyn. and Hydraul. Engrg., Techn. Univ. Denmark

14. Olesen, K.W. 1982
Introduction of streamline curvature into flow computation for shallow river bends.
Delft Univ.of Tech., Dept. of Civil Engng., Lab. Fluid Mech., Int. Rep. no. 5-82

15. Parker, G. 1976
On the cause and characteristic scales of meandering and braiding in rivers.
J. Fluid Mech., vol. 76, part 3, pp. 457-80

16. Rozowski, I.L. 1957
Flow of water in bends of open channels.
Academy of Sciences of the Uprainian SSR. Inst. Hydrol. and Hydraul. Engng. Also: Israel Program for Scientific Translation, Jerusalen 1961

17. Vriend, H.J. de. 1977
A mathematical model of steady flow in curved shallow channels.
J. Hydraul. Res., 15, no. 1

18. Vriend, H.J. de. 1978
Developing laminar flow in curved rectangular channels.
Delft Univ. of Tech., Dept. of Civil Engng., Lab. Fluid Mech., Int. Rep. no. 6-78

19. Vriend, H.J. de. 1979
Steady turbulent flow in curved rectangular channels.
Delft Univ. of Tech., Dept. of Civil Engng., Lab. Fluid Mech., Int. Rep. no. 5-79

20. Vriend, H.J. de. 1981a
Steady flow in shallow channel bends.
Delft Univ. of Tech., Dept. of Civil Engng., Communication on Hydraul. (also presented as doctoral thesis to the Delft Univ. of Tech.)

21. Vriend, H.J. de. 1981b
Velocity redistribution in curved rectangular channels.
J. Fluid Mech., vol. 107, pp. 423-39

22. Wang, D.G. 1981
Three-dimensional phenomena in straight flumes with mobile bed:
Filtering of sandflume data.
Delft Hydraul. Lab., TOW-inf. R657-XXXVI,R657/M1314, Sept.

23. Wang, D.G. & Klaassen, G.J. 1981
Three-dimensional phenomena in straight flumes with mobile bed:
Some results of filtering of bedlevel seconds and preliminary conclusions.
Delft Hydraul. Lab., TOW-inf. R657-XXXV,R657/M1314, July

24. Yalin, M.S. 1964
Geometrical properties of sand waves.
J. Hydraul. Div., Proc. ASCE, vol. 90, no. HY5

25. Yen, B.C. 1965
Characteristics of subcritical flow in a meandering channel.
Inst. of Hydraul. Res., Univ. of Iowa, Iowa City

26. Zimmerman, C. and Kennedy, J.F. 1978
Transverse bed slopes in curved alluvial streams.
J. Hydraul. Div., Proc. ASCE, vol. 104, no. HY1

Appendix A

Secondary flow inertia (De Vriend, 1981a)

The model for secondary flow inertia is based on numerical computations of the decaying flow beyond a bend. The governing equations for the flow can be considerably simplified and still not cease to describe the essential problem. The shallow water approximation (i.e. neglect lateral diffusion) and considering straight depth averaged streamlines only make it possible to disregard all y-derivatives except the transverse pressure gradient. If furthermore the pressure is assumed hydrostatically distributed, then the transverse momentum equation can be reduced to

$$u \frac{\partial v}{\partial x} = - \frac{1}{\rho} \frac{\partial p}{\partial y} + \frac{\partial}{\partial z} \left(A_t \frac{\partial v}{\partial z} \right) \qquad \text{(A1)}$$

in which A_t is the eddy viscosity and u and v are here dimensional local velocities, i.e. u(x,y,z) and v(x,y,z).

In stead of solving the longitudinal momentum equation a similarity approximation is assumed to apply to the longitudinal flow velocity, namely

$$u = \bar{u} f_u \qquad \text{(A2)}$$

in which the bar denotes a depth averaged quantity. The function f_u is given by

$$f_u = 1 + \frac{\sqrt{f}}{\kappa} \left(1 + \ln \frac{z}{h} \right) \qquad \text{(A3)}$$

The distribution of the eddy viscosity (A4) is the well known parabolic distribution, which is consistend with the logarithmic velocity profile,

$$A_t = \kappa \sqrt{f} \bar{u} \frac{z}{h} \left(1 - \frac{z}{h} \right) \qquad \text{(A4)}$$

Inserting eqs. (A2) and (A4) into eq. (A1) the transverse momentum equation can be written as

$$f_u \frac{\partial v'}{\partial x'} = \frac{\partial p'}{\partial y'} + \frac{\partial}{\partial z'} \left(A_t' \frac{\partial v'}{\partial z'} \right) \qquad \text{(A5)}$$

in which

$v' = v/\bar{u}$
$A_t' = z'(1-z')$
$z' = z/h$
$y' = y/h$
$x' = \kappa \sqrt{f}\, x/h$
$p' = p/(\rho \bar{u} \kappa \sqrt{f})$

The dimensionless pressure gradient can be determined with the auxiliary condition of zero net flow in transverse direction (straight depth averaged streamlines)

$$\int_0^1 v' dz' = 0 \qquad \text{(A6)}$$

A known vertical distribution of v' (fully developed secondary flow) at the upstream end is applied as a boundary condition for eq. (A5)

$$v'|_{x=0} = v_0' \qquad \text{(A7)}$$

in which v_0' is the solution of

$$\frac{\partial}{\partial z'} \left(A_t' \frac{\partial v_0'}{\partial z'} \right) + \frac{\partial p'}{\partial y'} = - f_u^2 \frac{1}{\kappa \sqrt{f}} \qquad \text{(A8)}$$

At the surface the shear stress vanishes

$$A_t' \frac{\partial v'}{\partial z'} \Big|_{z'=1} = 0 \qquad \text{(A9)}$$

- and at the bottom the wall function approximation is applied

$$v' = \frac{v_t'}{\kappa} \left\{ \frac{\kappa}{\sqrt{f}} + 1 + \ln z' \right\} \qquad \text{(A10)}$$

The set of equations (A5 - A7 and A9-A10) is solved numerical (details, see de Vriend, 1981a). In fig. A1 the secondary flow intensity

$$I_{sec} = \int_0^1 /v'/dz' \qquad (A11)$$

- is plotted versus the dimensionless longitudinal coordinate x' on semi-logarithmic paper. The figure shows that the secondary flow intensity decrease approximately exponential with x'. I.e.

$$I_{sec}(x') \simeq I_{sec}(0) \exp(-\frac{x'}{\lambda}) \qquad (A12)$$

in which the relaxation length λ appeared to be almost independend of the roughness coefficient f. In terms of dimensional variables the secondary flow intensity beyond a bend can therefore very well be approximated by

$$I_{sec}(x) = I_{sec}(0) \exp(-\frac{\sqrt{f}}{1.3}\frac{x}{h}) \qquad (A13)$$

In case of a varying source term it is analogous assumed that the secondary flow inertia can be found from

$$\frac{1.3}{\sqrt{f}} h \frac{\partial I_{sec}}{\partial x} + I_{sec} = SOURCE(x) \qquad (A14)$$

If in addition a similarity hypothesis is applied to the secondary flow; then the relaxation length $(1.3\ h/\sqrt{f})$ applies to the transverse bed shear stress as well, because in this case the shear stress is assumed proportional to the secondary flow intensity.

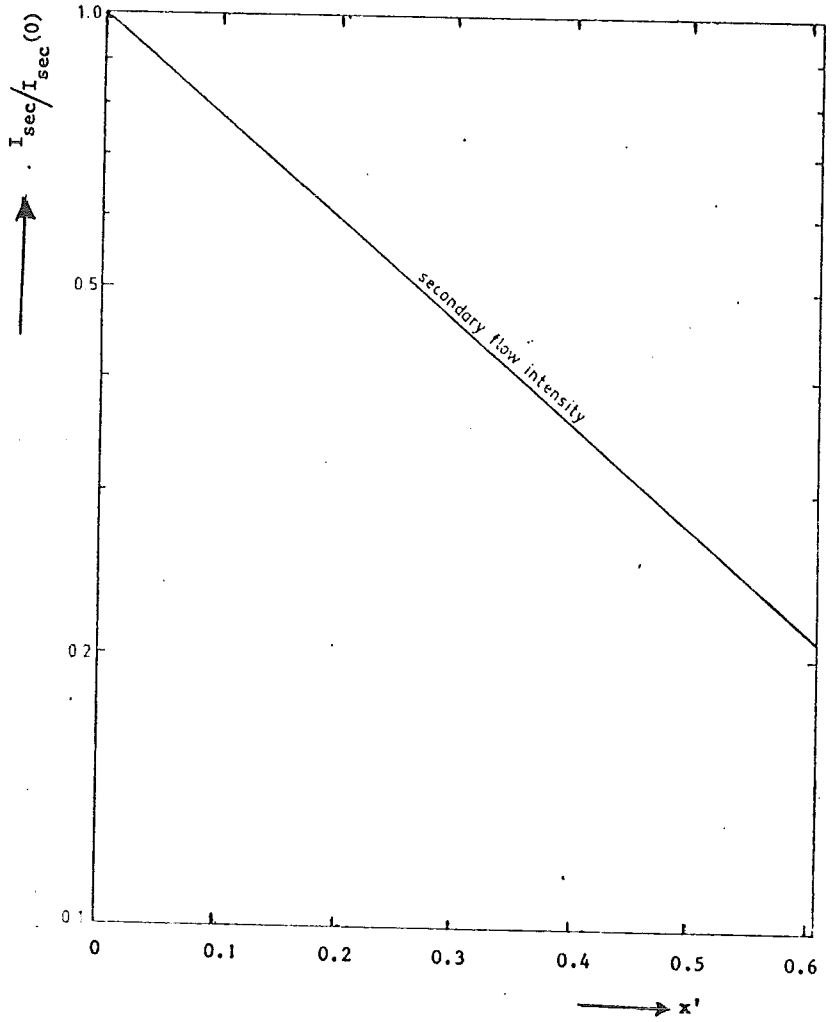

Figure A1. Decay of secondary flow intensity beyond a bend. C = 50 $m^{\frac{1}{2}}/s$ (After De Vriend, 1981a).

TEST	Q (m^3/s)	W (m)	h (m)	S (kg/h)	F (-)	θ (-)	f (10^{-2})	l (-)	H[1] (-)	k_w (-)
T04	0.075	1.50	0.111	63.7	0.432	0.214	1.28	0.55	0.57	0.23
T12	0.090	1.50	0.115	127.1	0.491	0.307	1.37	0.58	0.53	0.24
T14	0.063	1.50	0.105	13.7	0.394	0.0925	0.70	0.41	0.45	0.22
T19	0.100	1.50	0.087	577.8	0.830	0.485	1.00	0.54	0.51	0.18
T23	0.146	1.50	0.200	65.0	0.346	0.259	1.32	0.67	0.35	0.42
T24	0.266	1.50	0.301	125.3	0.341	0.379	1.33	0.69	0.25	0.63
T26	0.401	1.50	0.405	179.1	0.331	0.501	1.39	(0.66)	(0.21)	(0.85)
T31	0.131	1.125	0.208	48.6	0.392	0.266	1.03	0.60	0.26	0.44
T34	0.048	0.50	0.211	23.6	0.316	0.281	1.65	-	-	-

[1] $H=H_{bar}/h$, H_{bar} is the mean height of the alternate bars.

Table 1. Sand flume data (Wang & Klaassen, 1981).

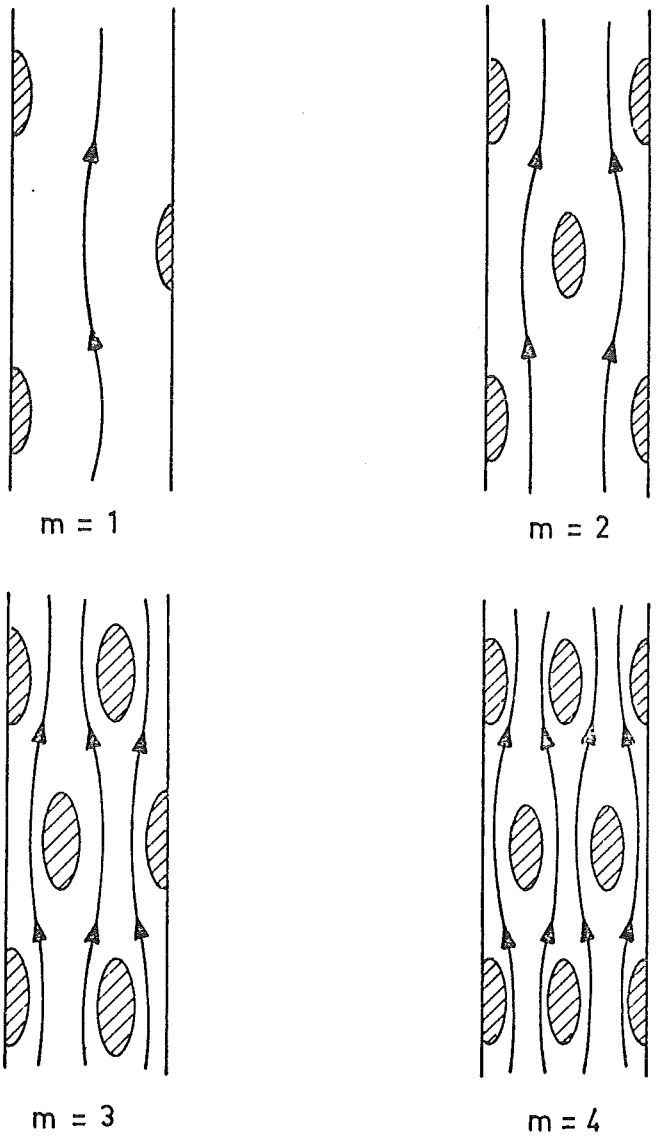

Figure 1. Bed patterns associated with different values of m. Submerged bars (shaded) and typical streamline patterns.

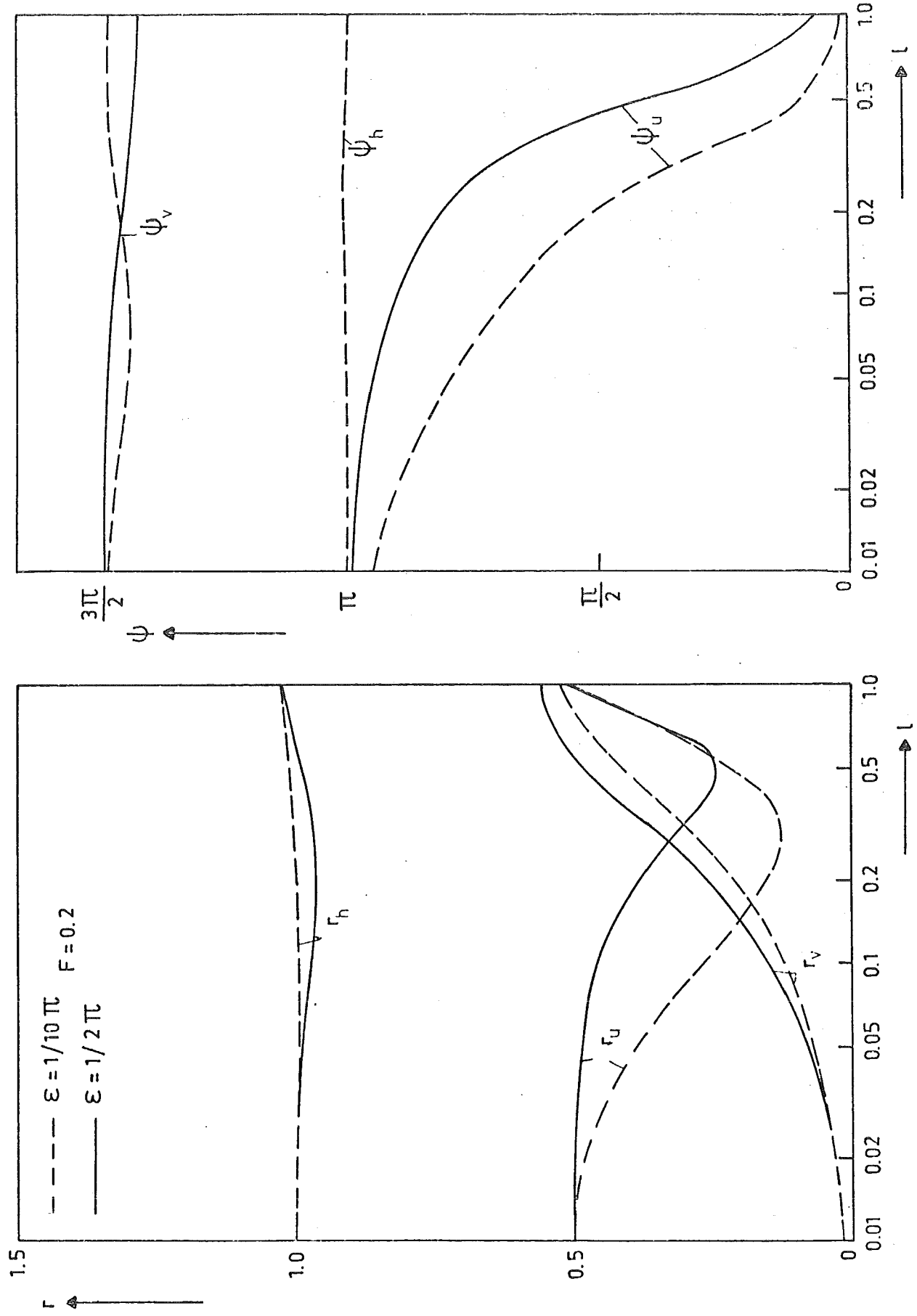

Figure 2. Phase lag (above) and amplitude (below) of depth (h), longitudinal and transverse velocity (u and v, respectively) for different values of ε.

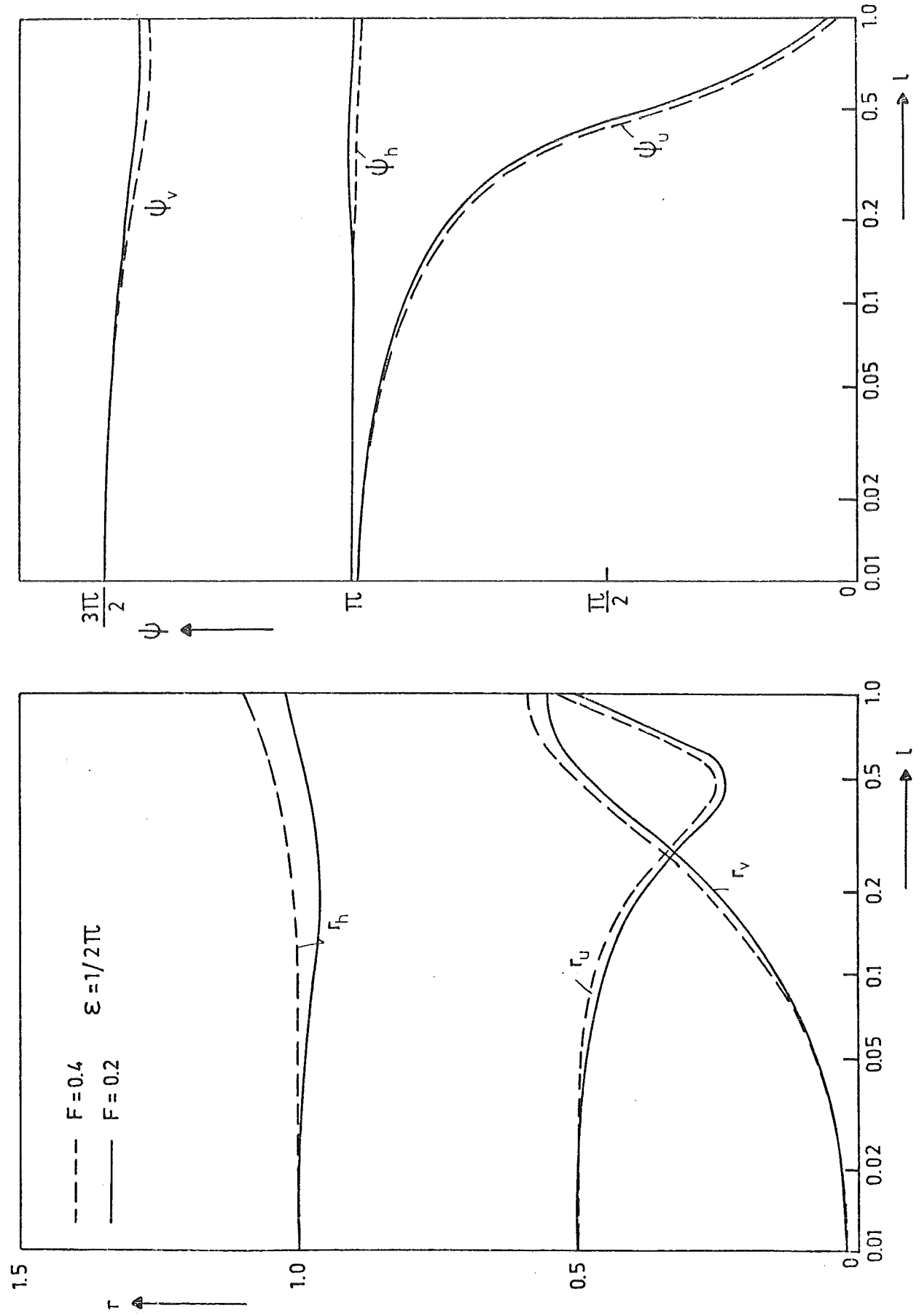

Figure 3. Phase lag (above) and amplitude (below) of depth (h), longitudinal and transverse velocity (u and v, respectively) for different values of the Froude number (F).

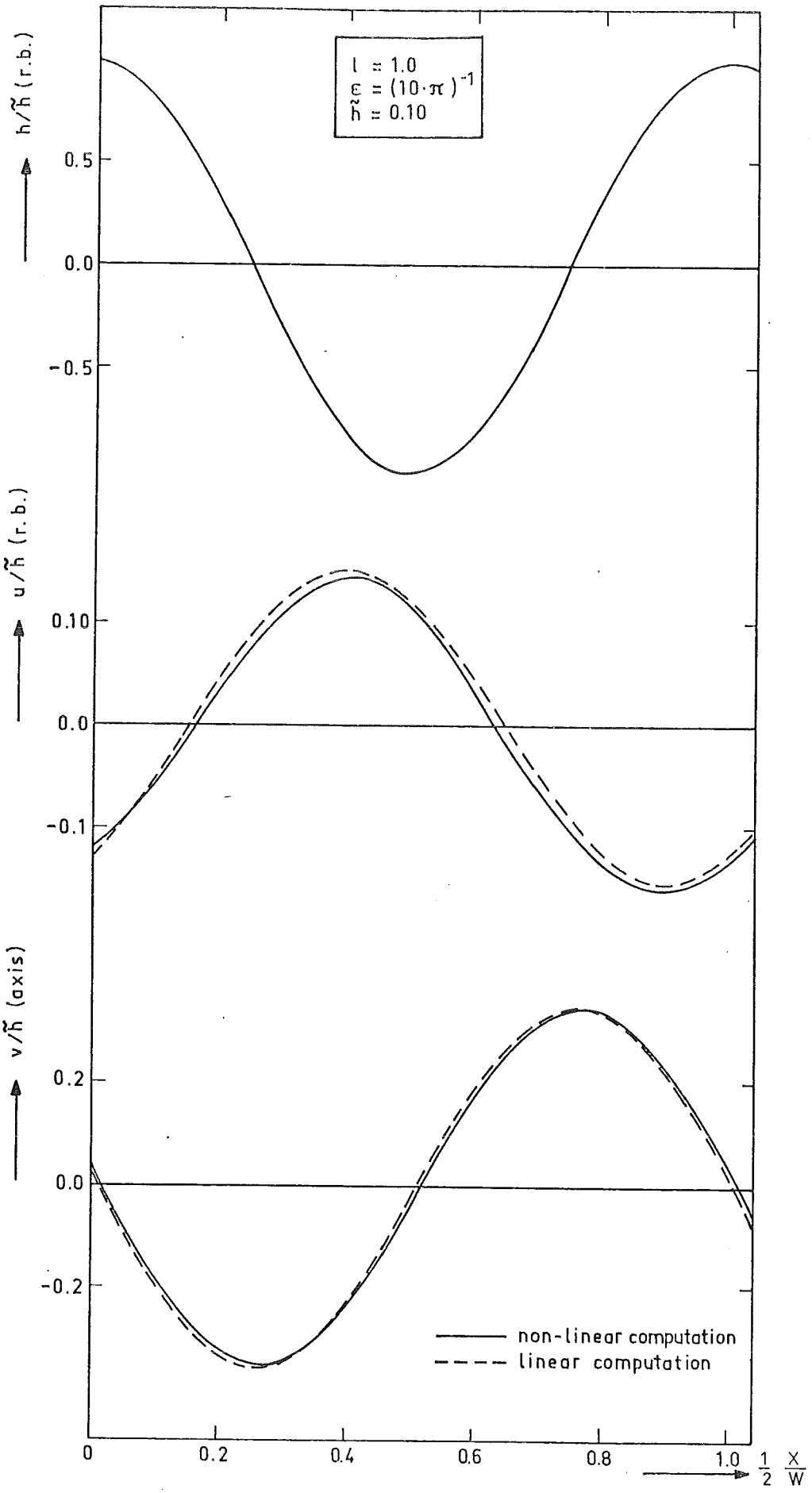

Figure 4. Linear and non-linear computation of the flow over submerged bars.

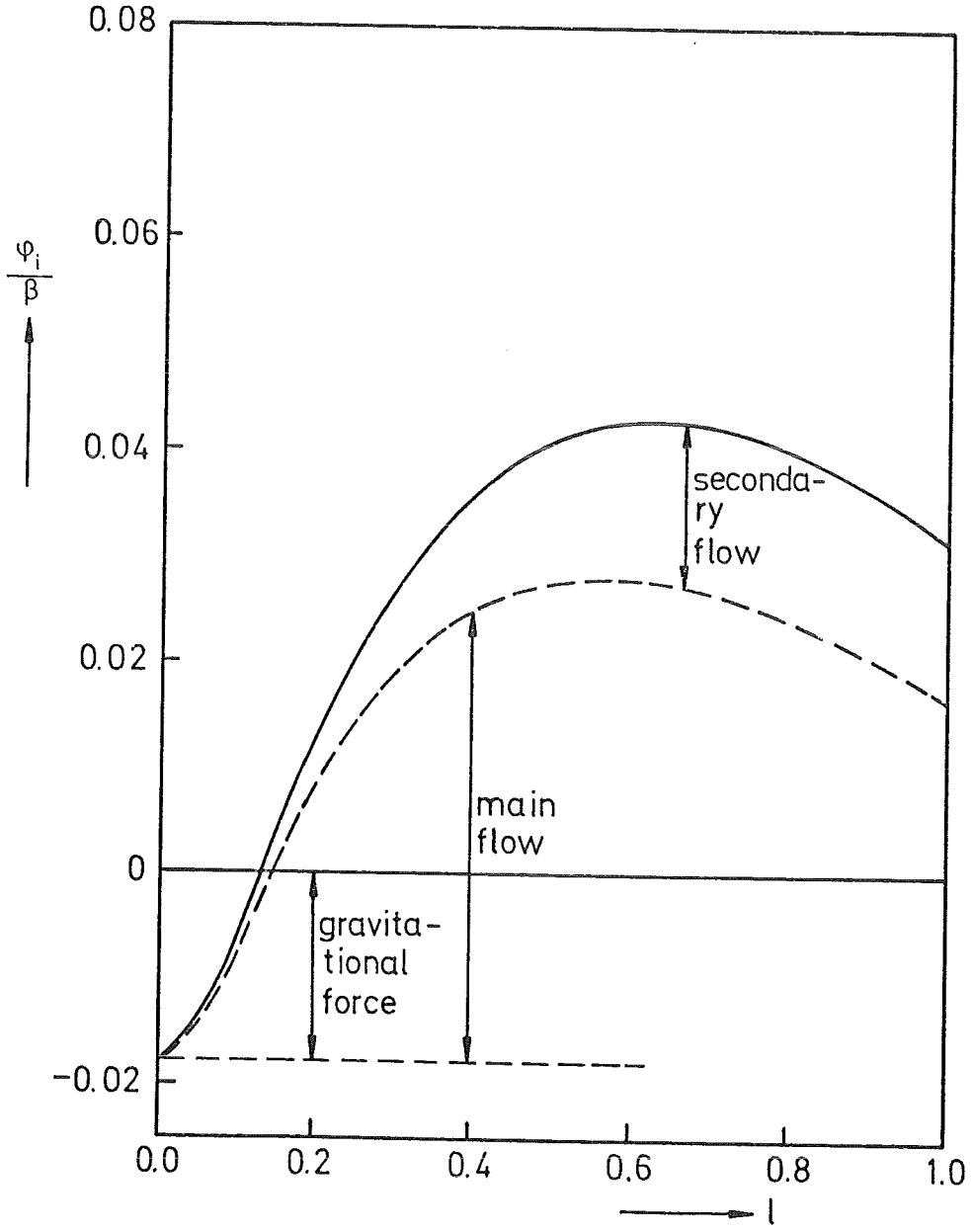

Figure 5. Amplification factor. Reference example.

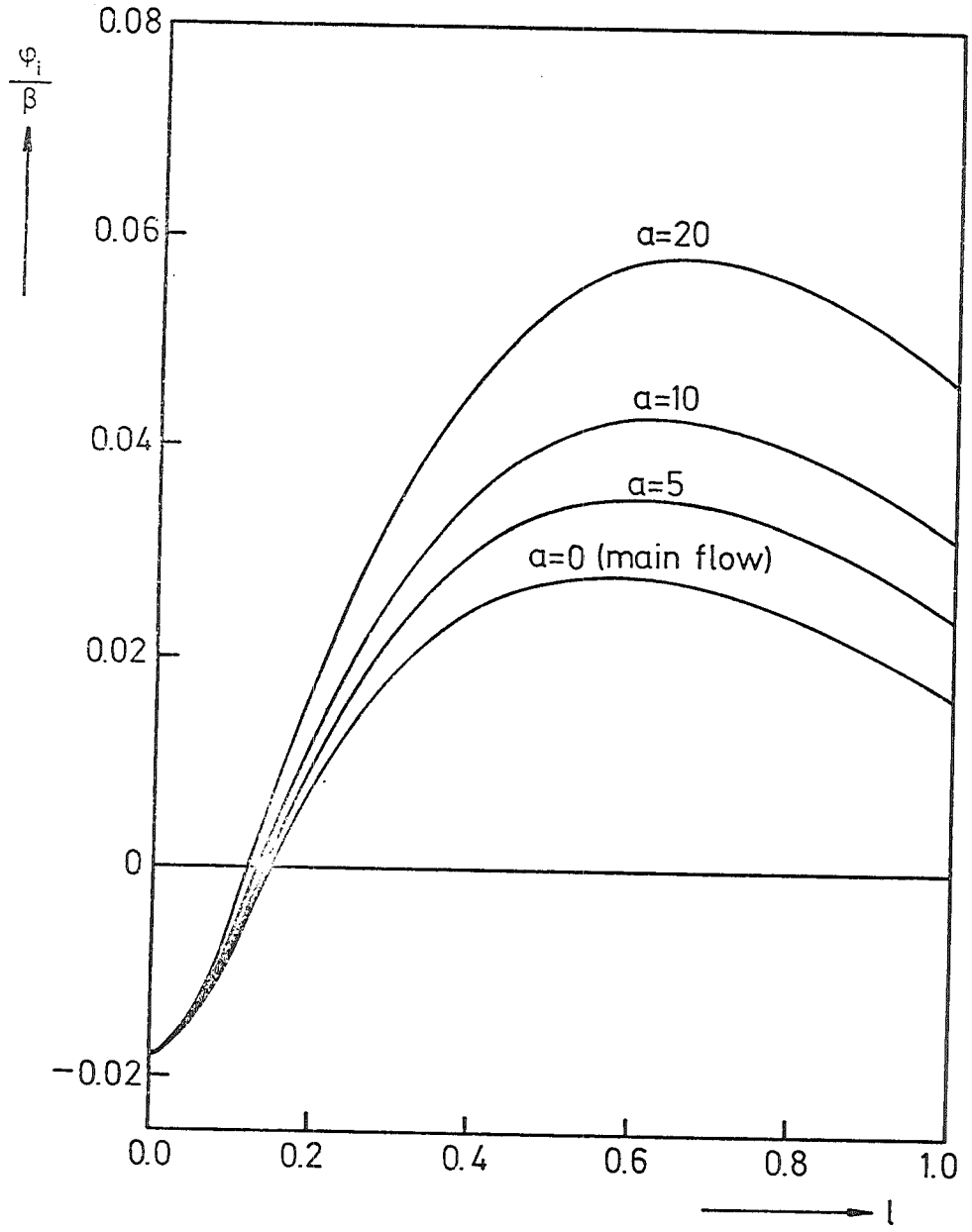

Figure 6. Amplification factor. Influence of magnitude of secondary flow.

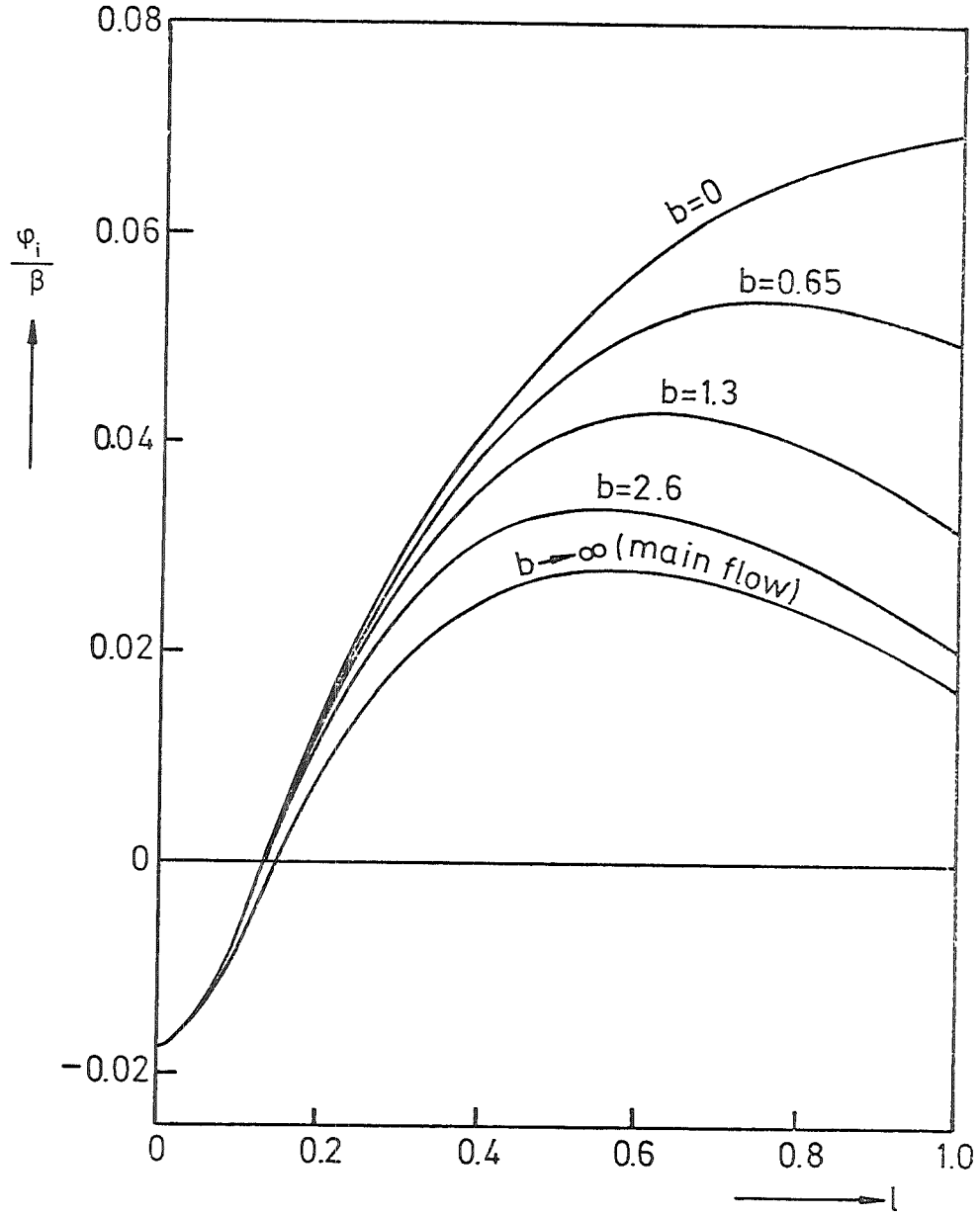

Figire 7. Amplification factor. Influence of secondary flow inertia.

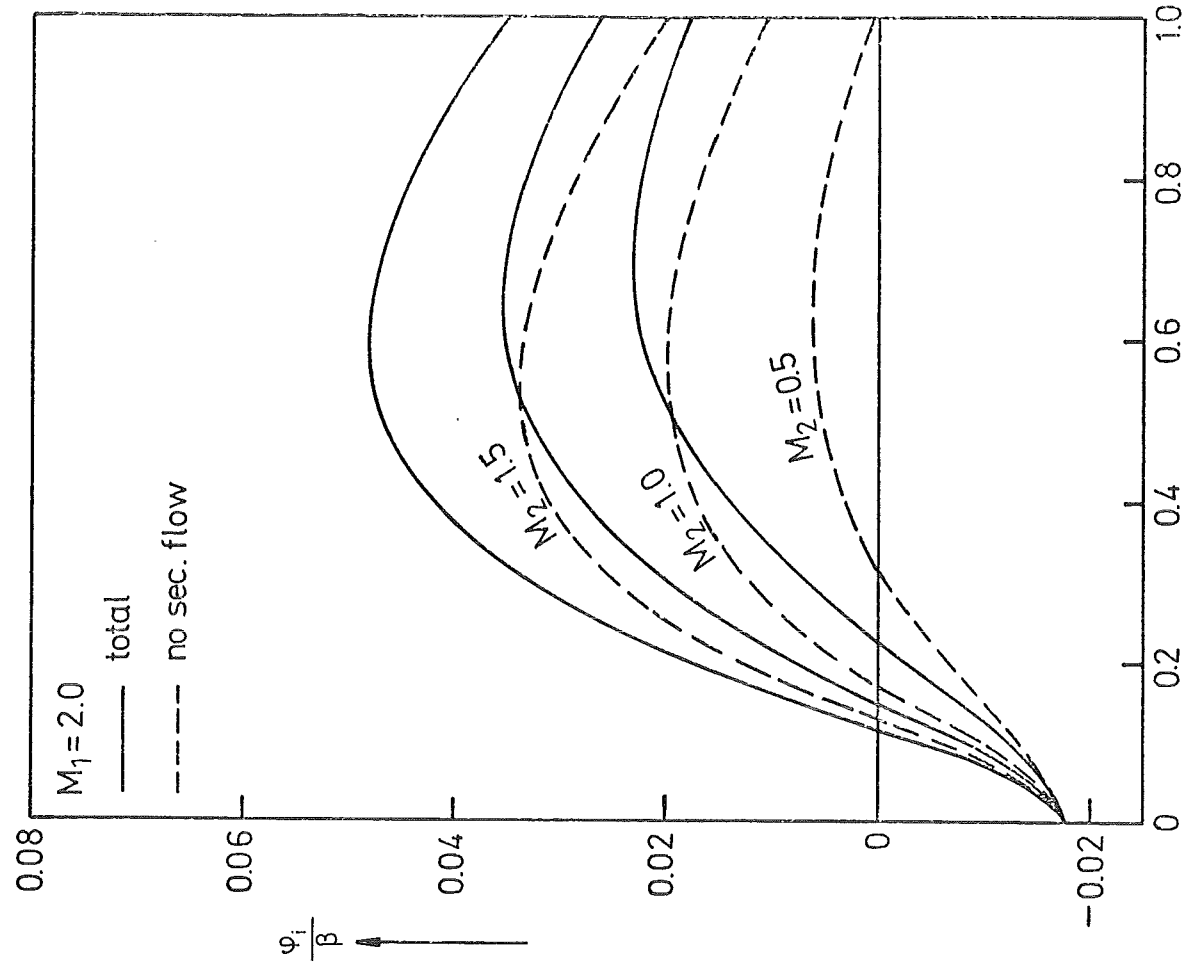

Figure 9. Amplification factor. Influence of model for the roughness coefficient (M_2).

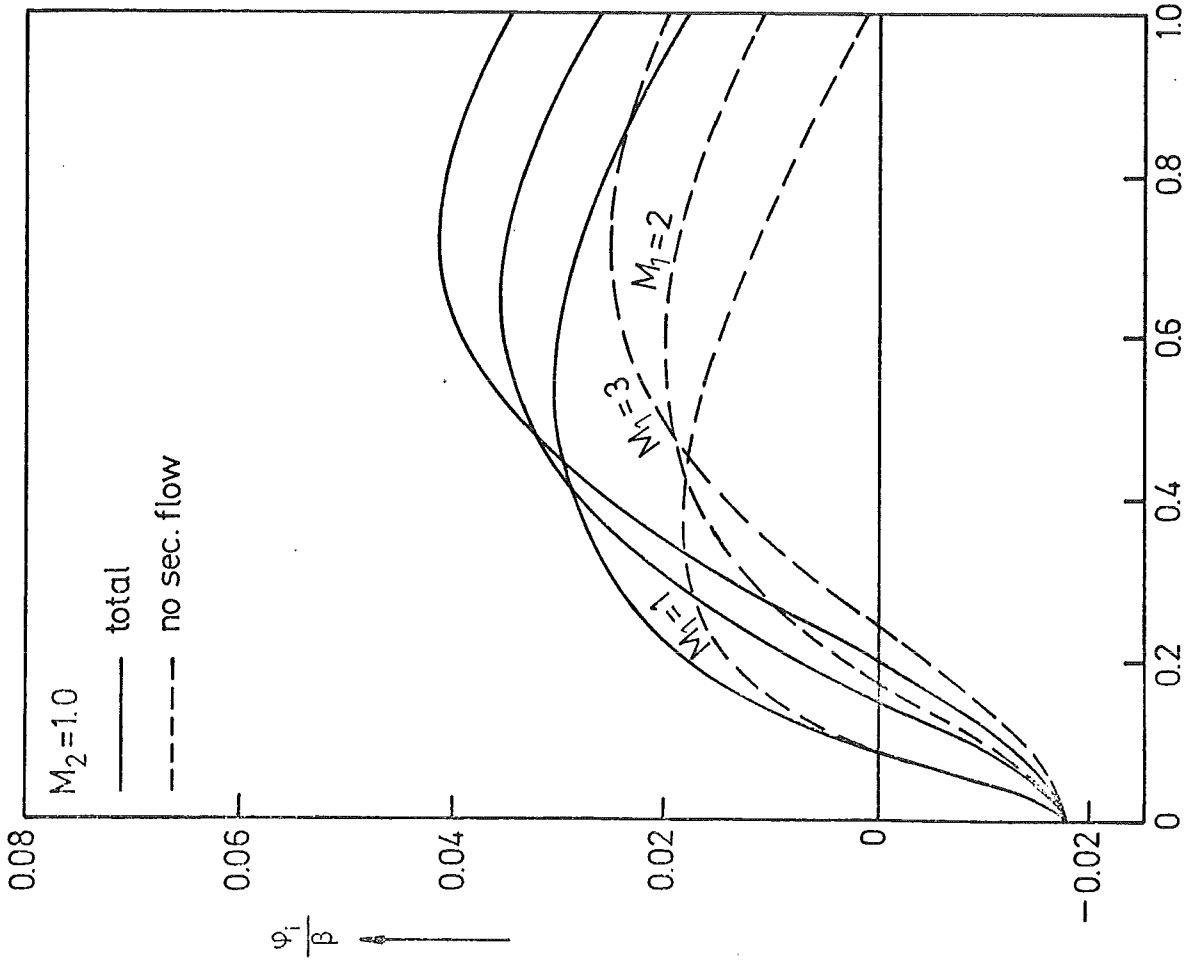

Figure 8. Amplification factor. Influence of model for the roughness coefficient (M_1).

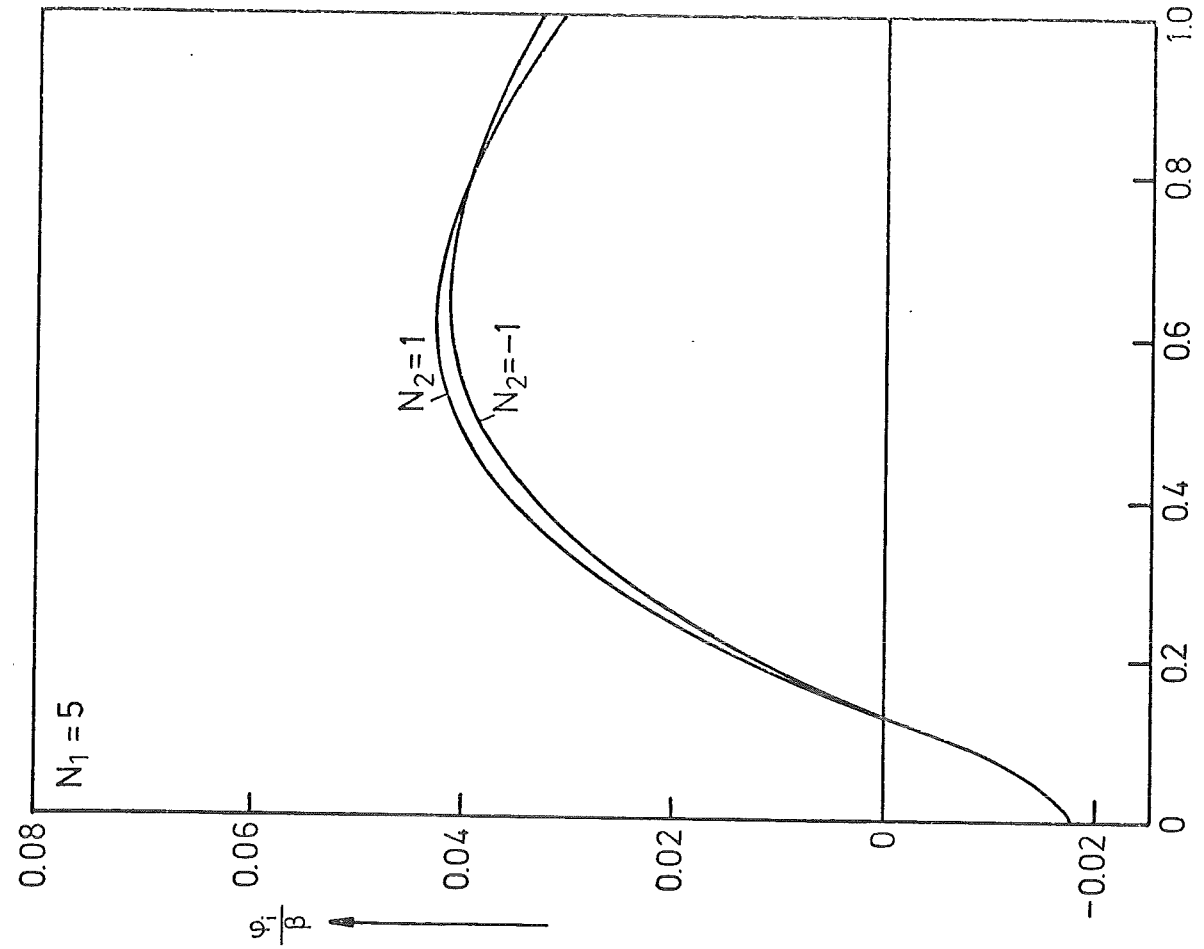

Figure 11. Amplification factor. Influence of model for the sediment transport (N_2).

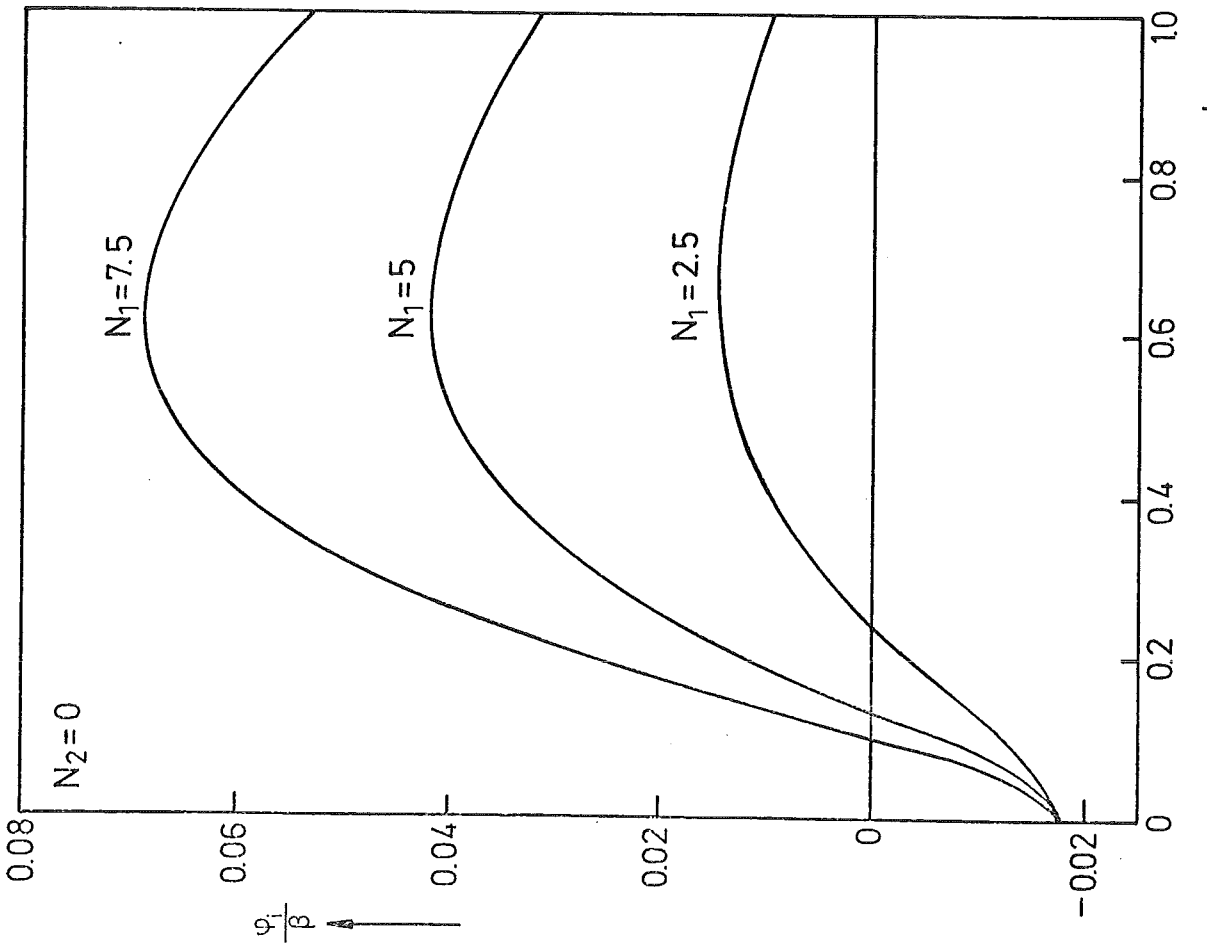

Figure 10. Amplification factor. Influence of model for the sediment transport (N_1).

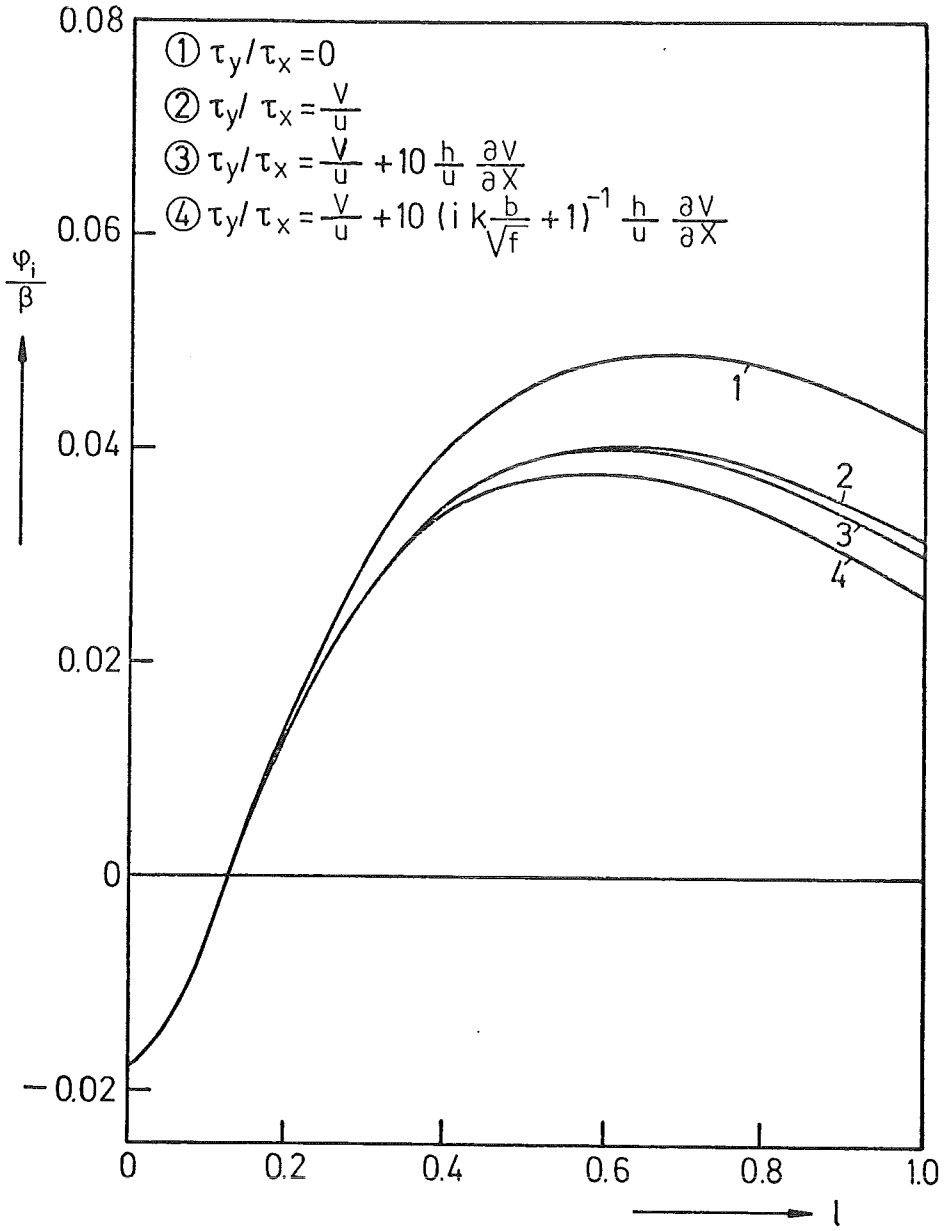

Figure 12. Amplification factor. Influence of different ways to account for the transverse bed shear stress in the flow model.

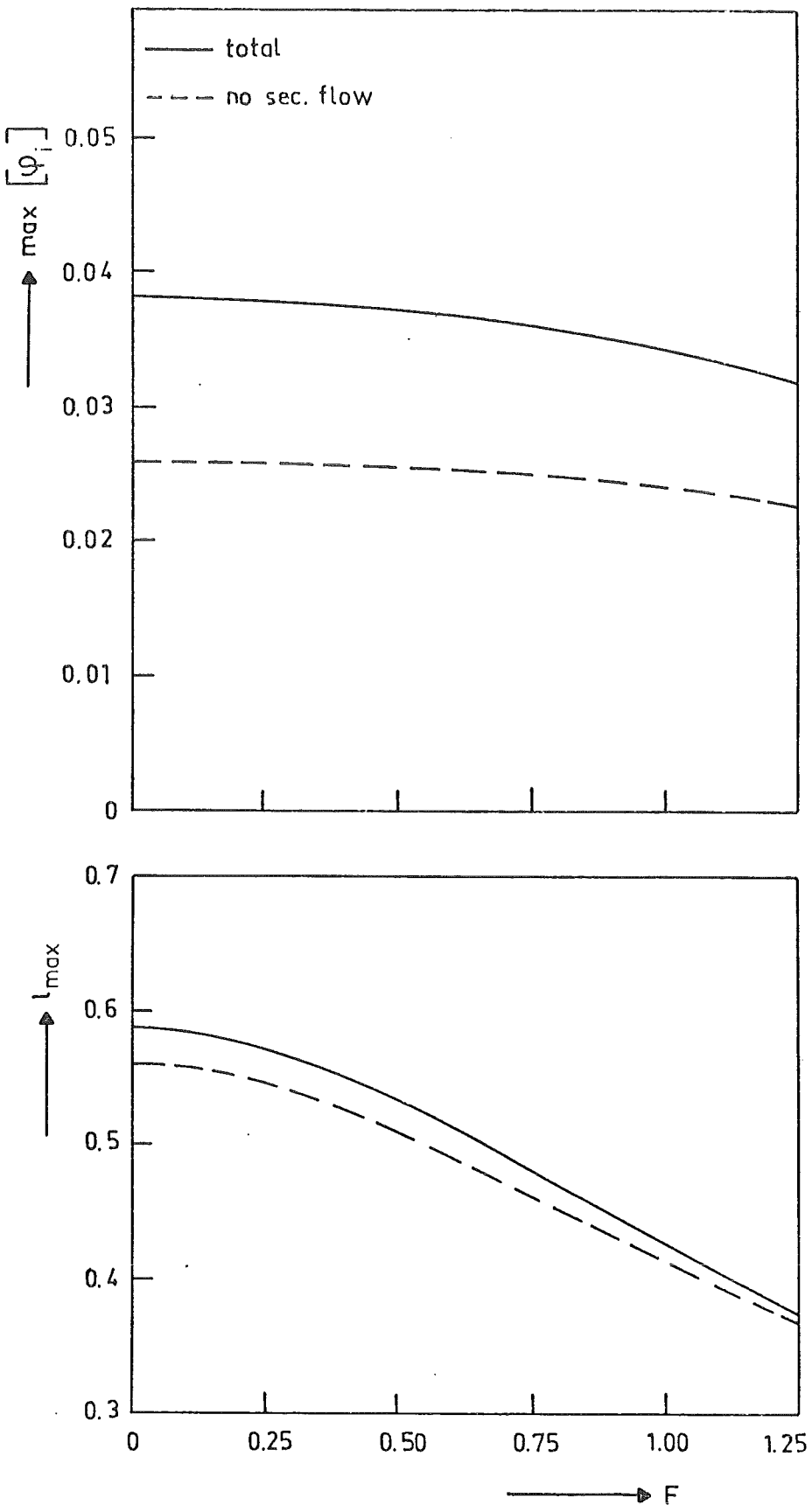

Figure 13. Maximum amplification factor. Influence of the Froude number (F).

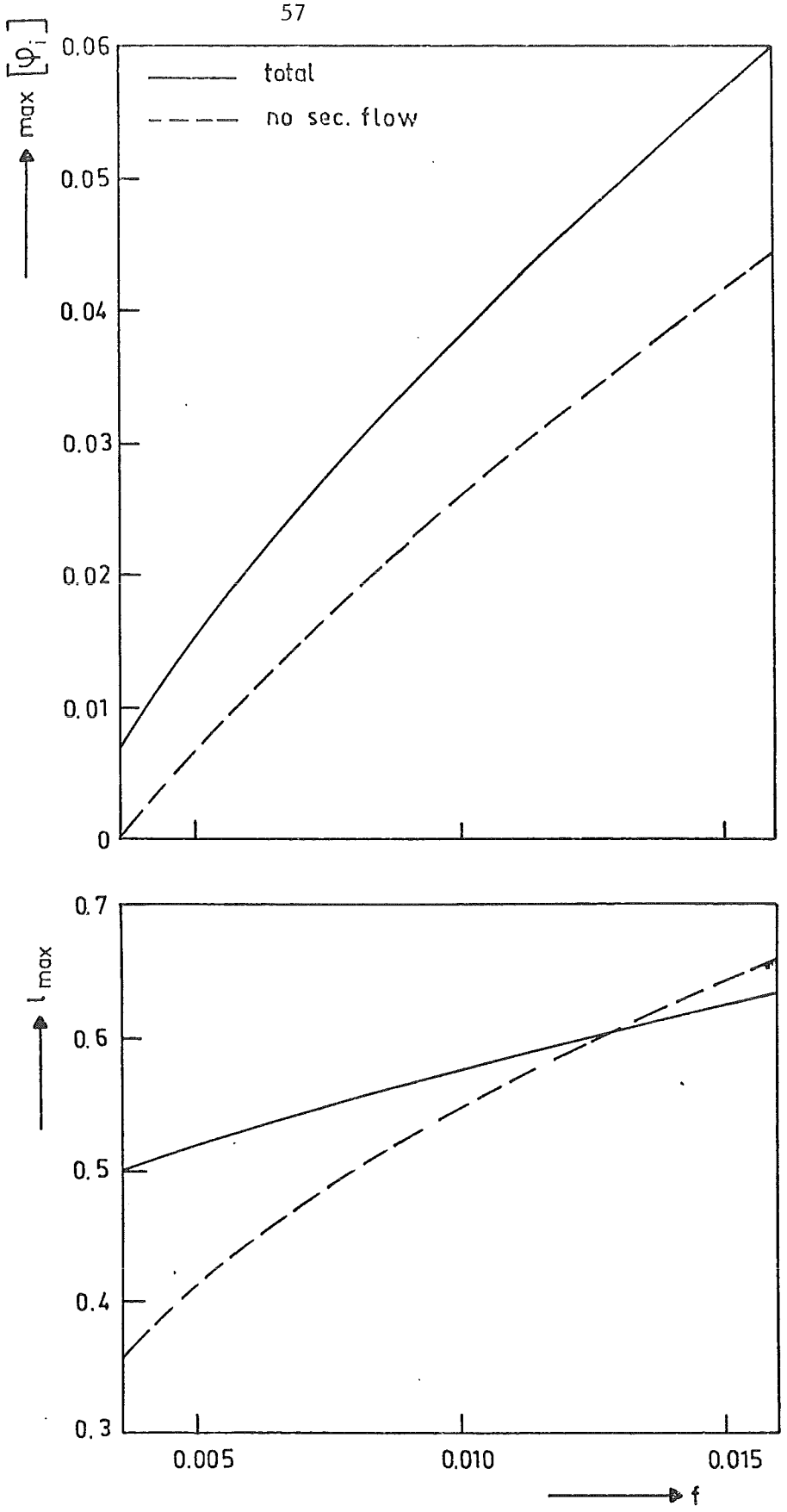

Figure 14. Maximum amplification factor. Influence of the roughness coefficient ($f = \frac{g}{C^2}$).

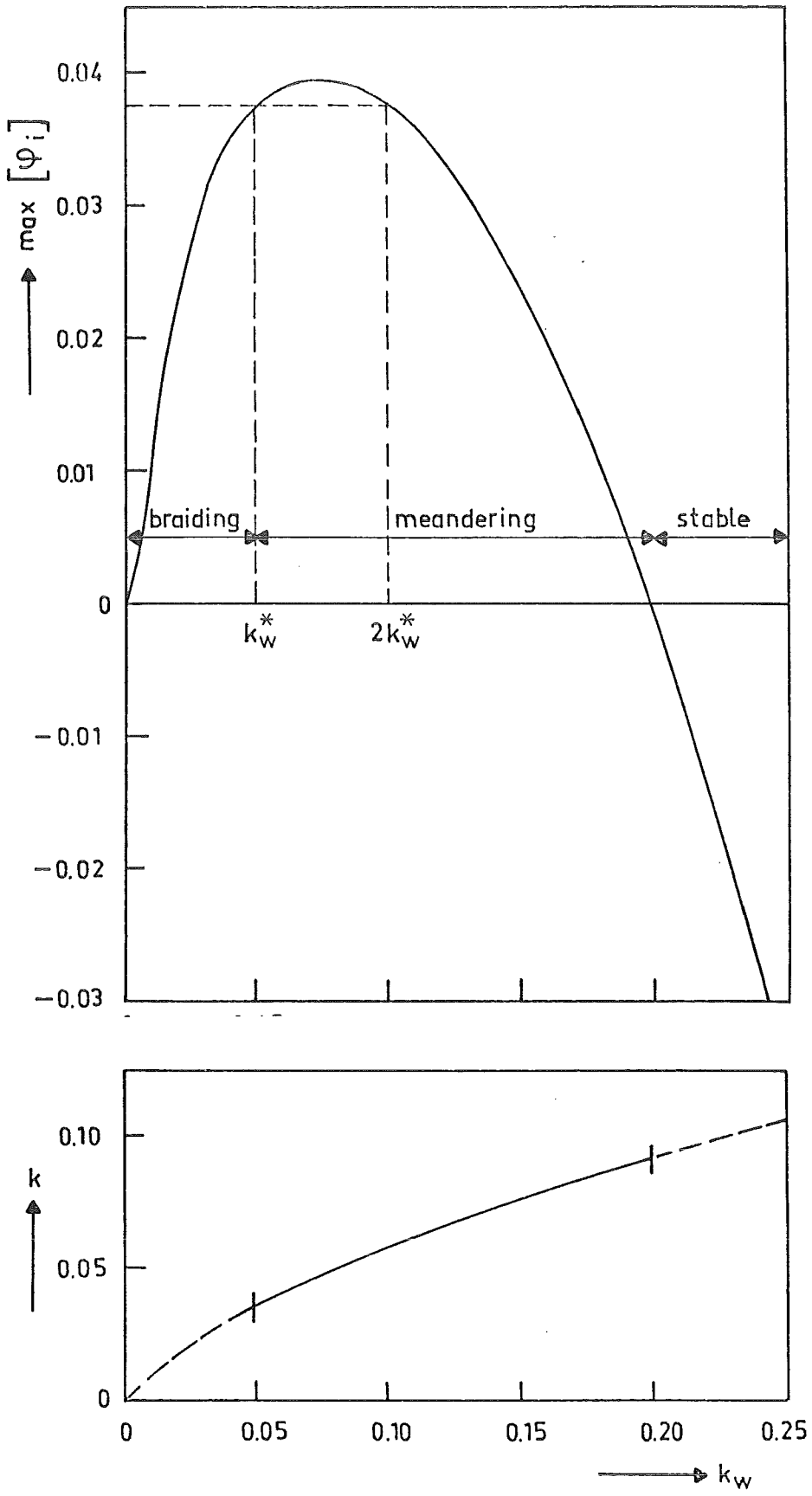

Figure 15. Maximum amplification factor. Influence of the width of the channel ($k_w = m \frac{\pi}{W}$).

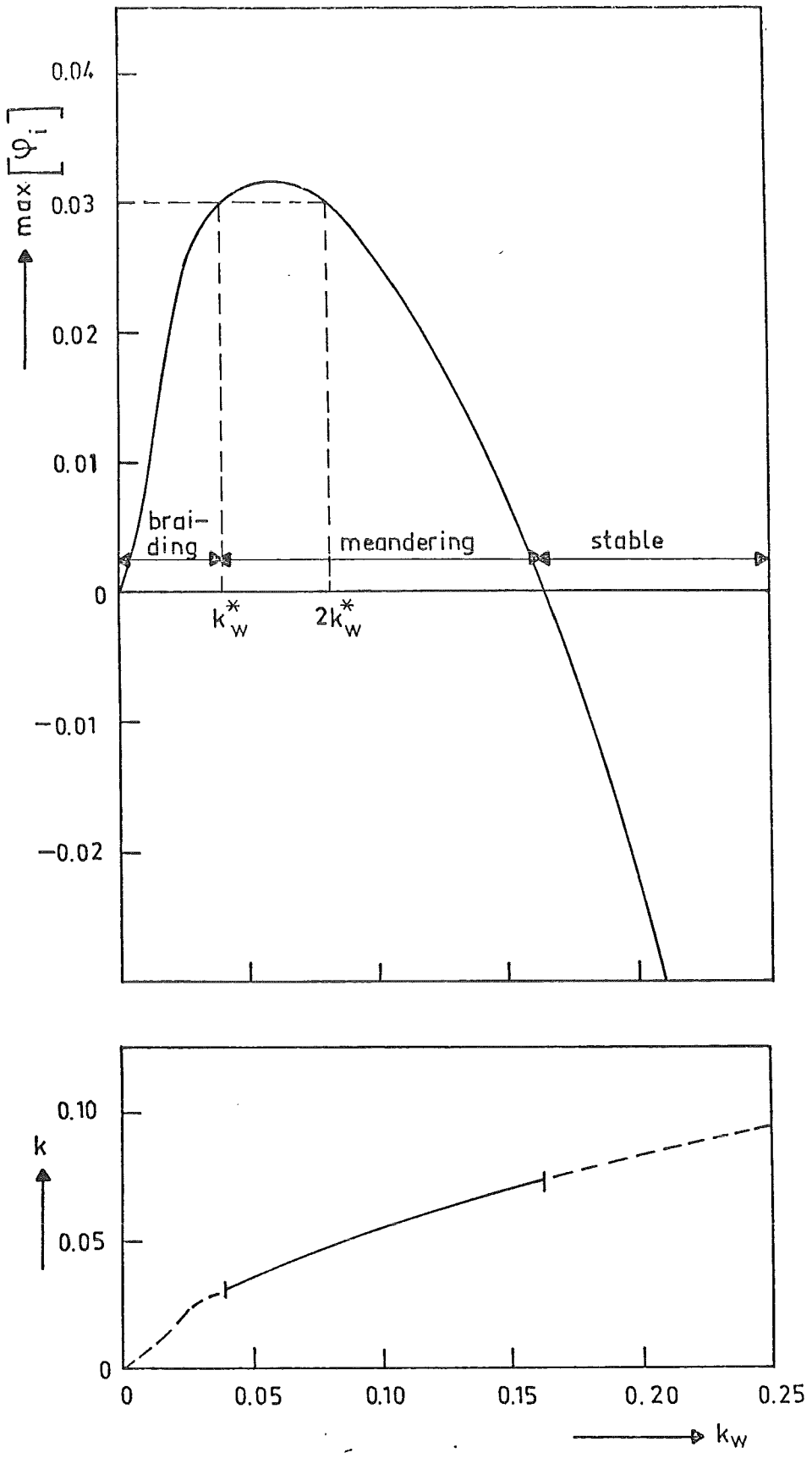

Figure 16. Maximum amplification factor. Influence of the width of the channel ($k_w = m \frac{\pi}{W}$). No secondary flow (a = 0).

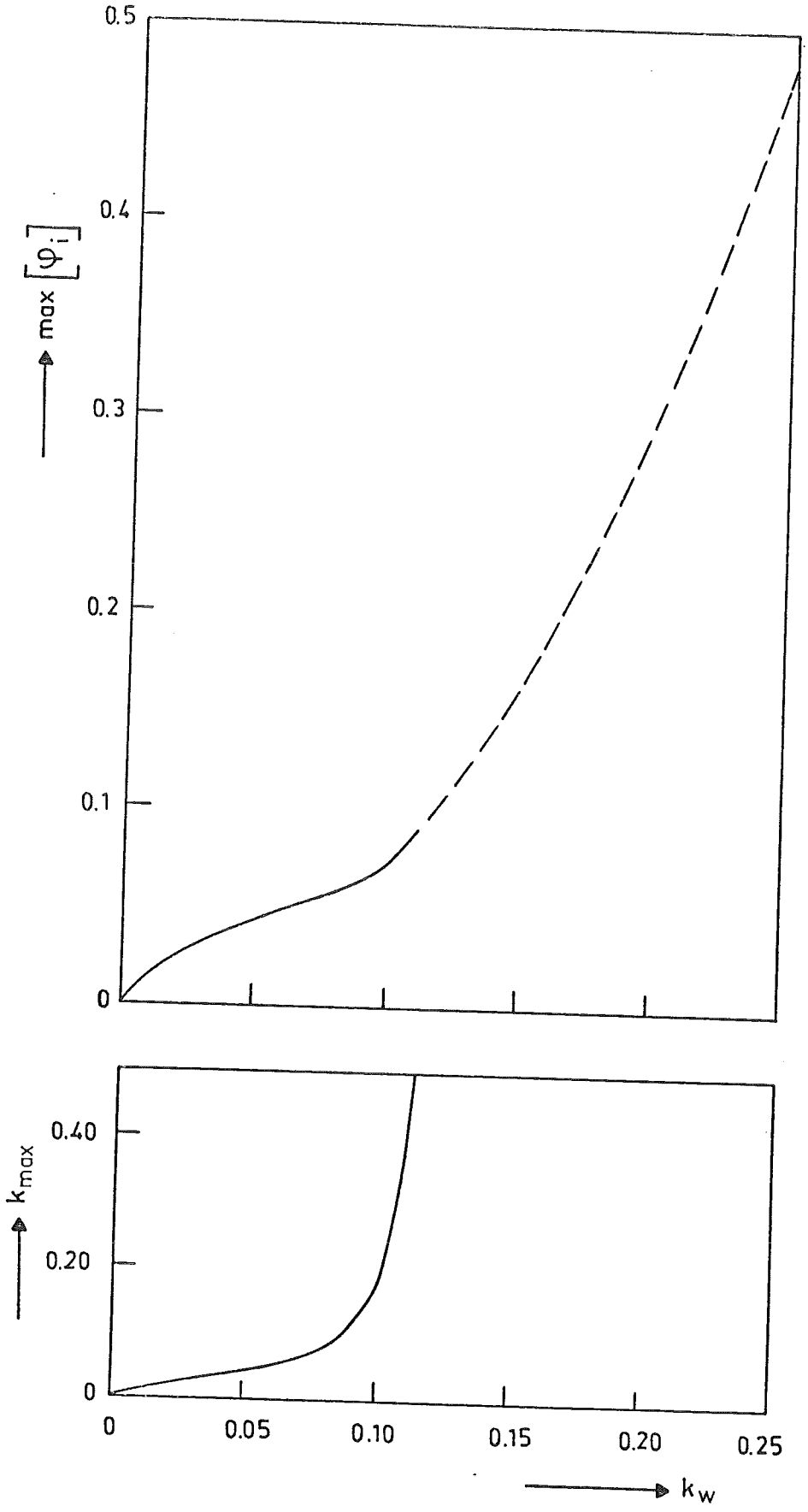

Figure 17. Maximum amplification factor. Influence of the width of the channel ($k_w = m \frac{\pi}{W}$). Secondary flow inertia neglected (b = 0).

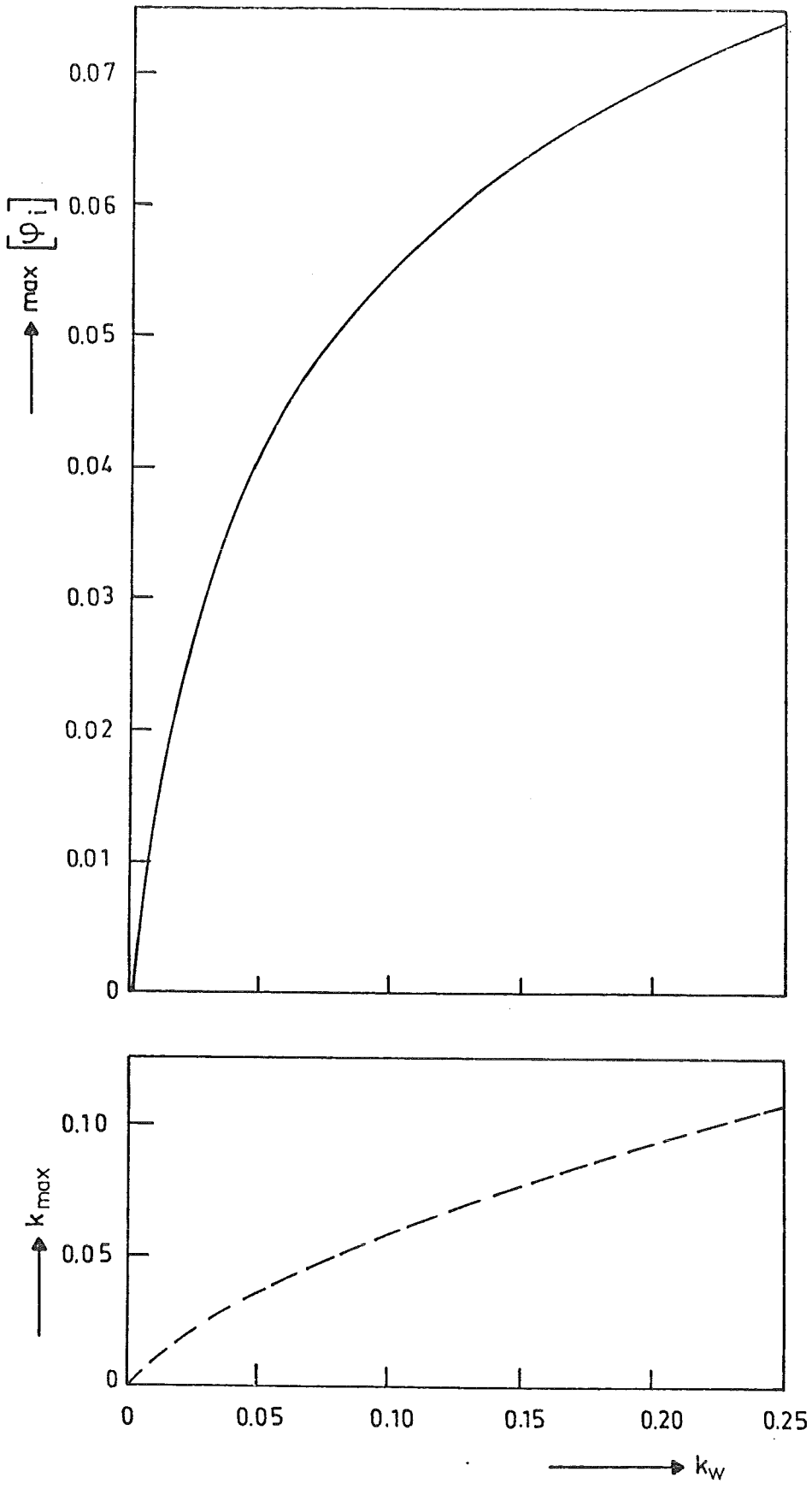

Figure 18. Maximum amplification factor. Influence of the width of the channel ($k_w = m \frac{\pi}{W}$). Gravitational force neglected ($c = 0$).

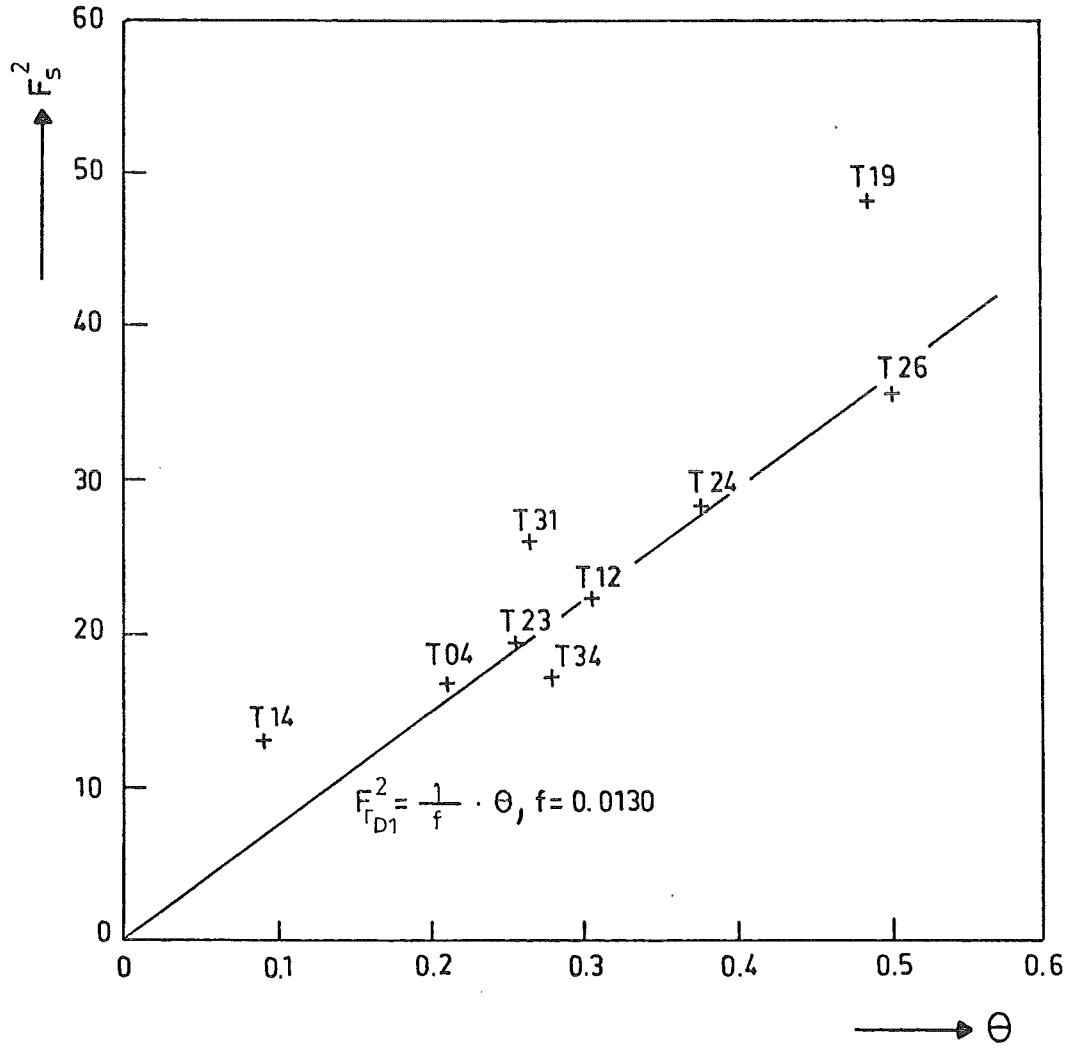

Figure 19. Bed shear stress (Shield parameter) as a function of the densimetric Froude number. Sand flume data.

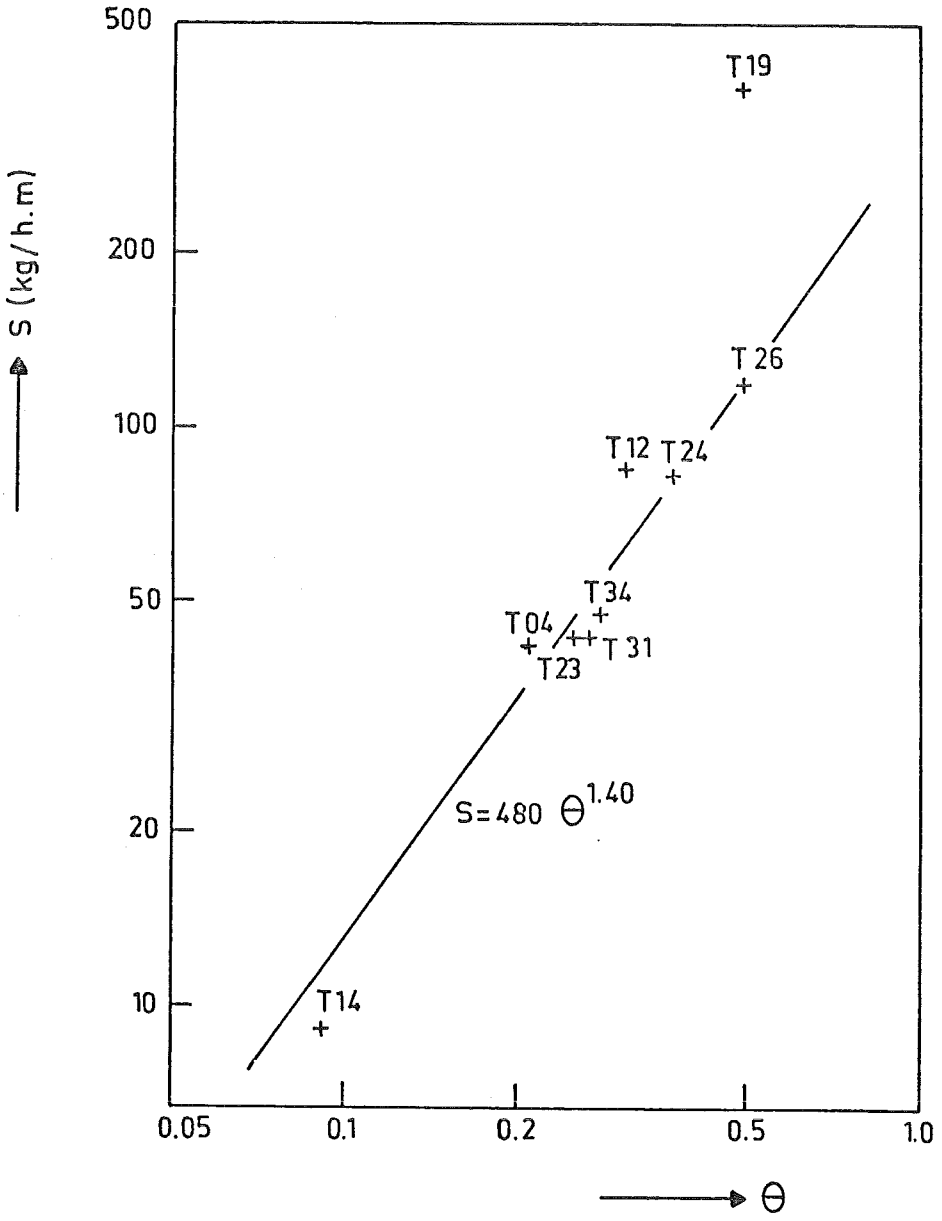

Figure 20. Transport rate as a function of the Shield parameter. Sand flume data.

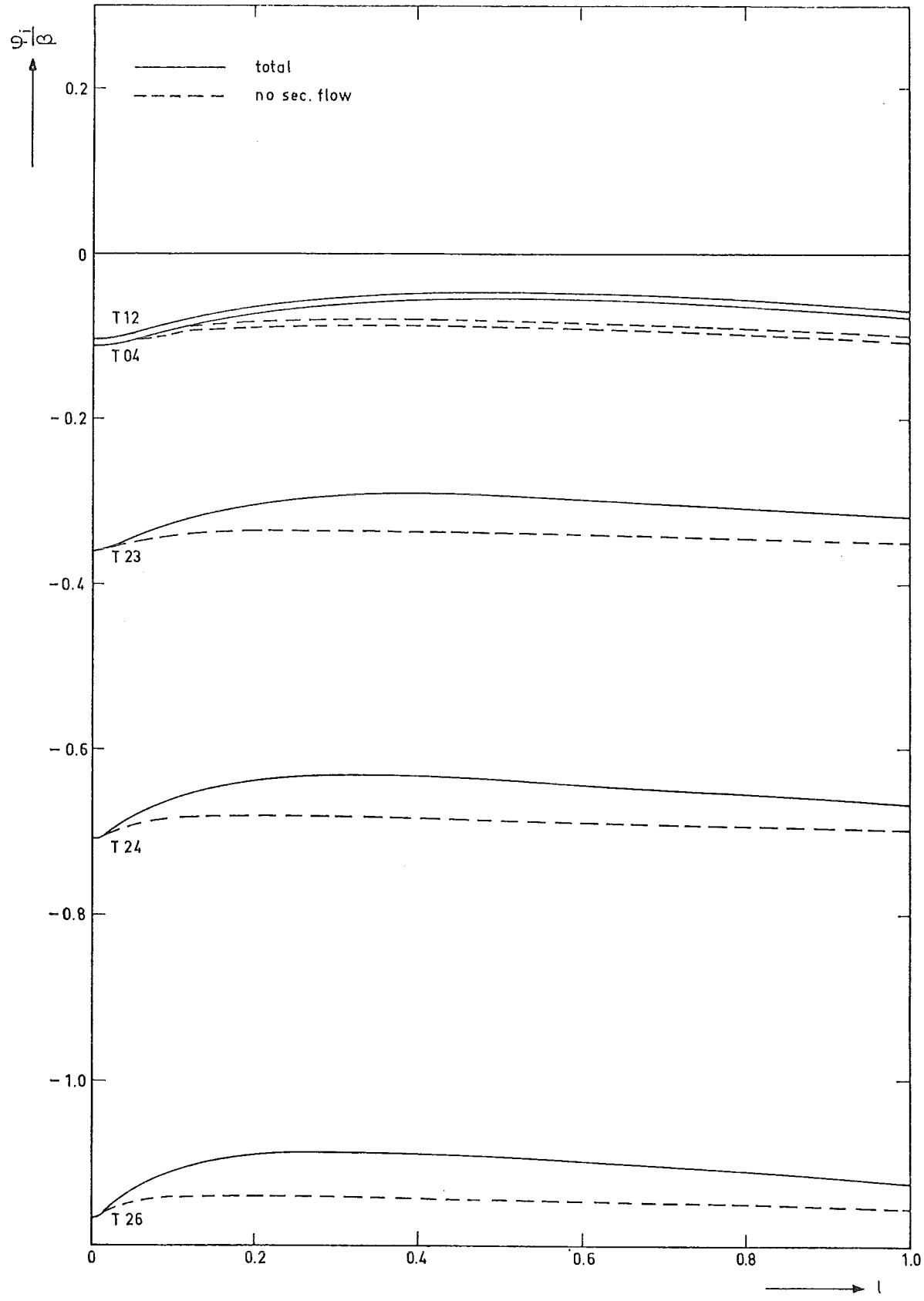

Figure 21. Amplification factor for the flume experiments.

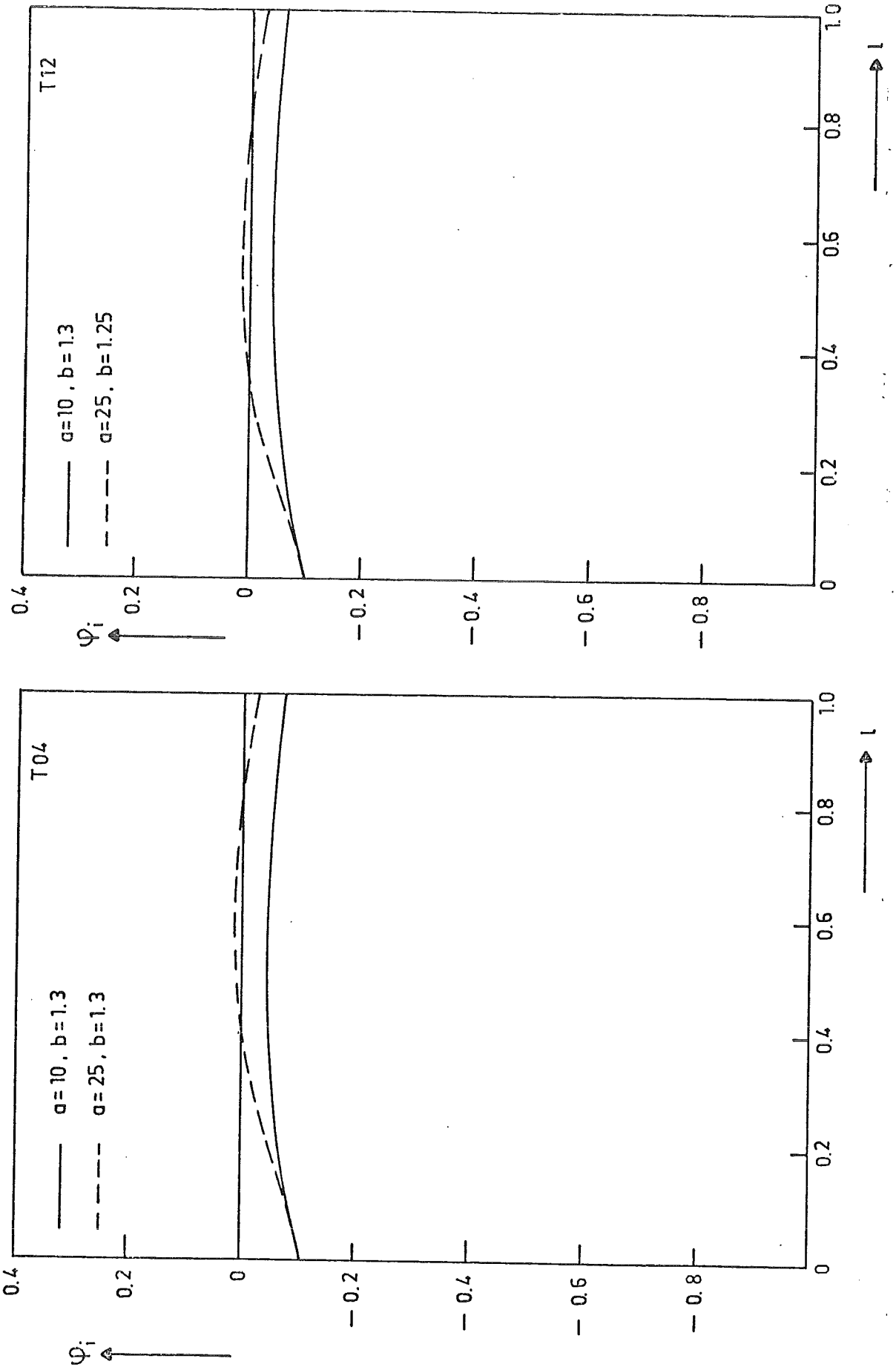

Figure 22a. Amplification factor for the flume experiments. Adapted secondary flow coefficients (a and b).

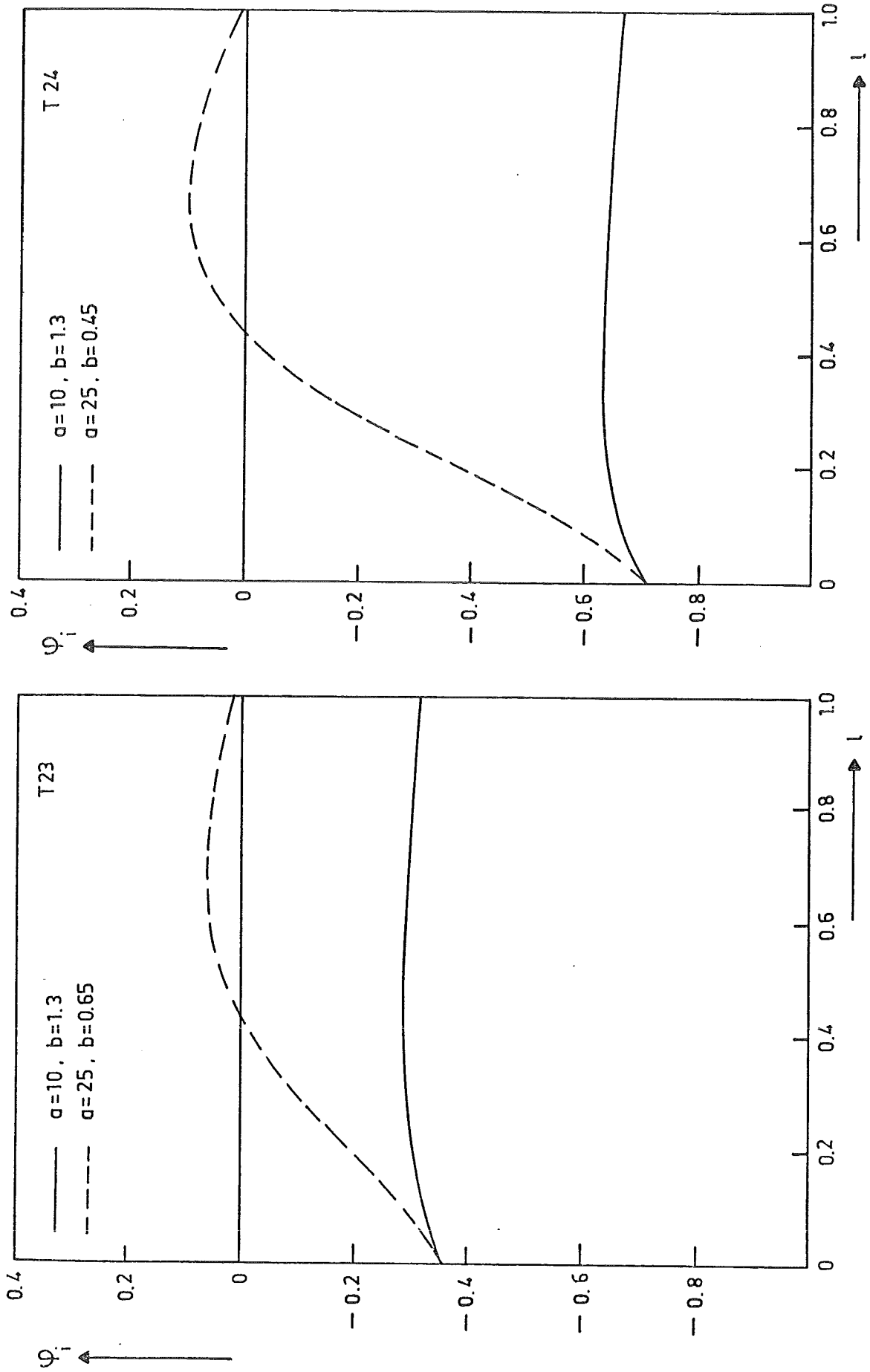

Figure 22b. Amplification factor for the flume experiments. Adapted secondary flow coefficients (a and b).

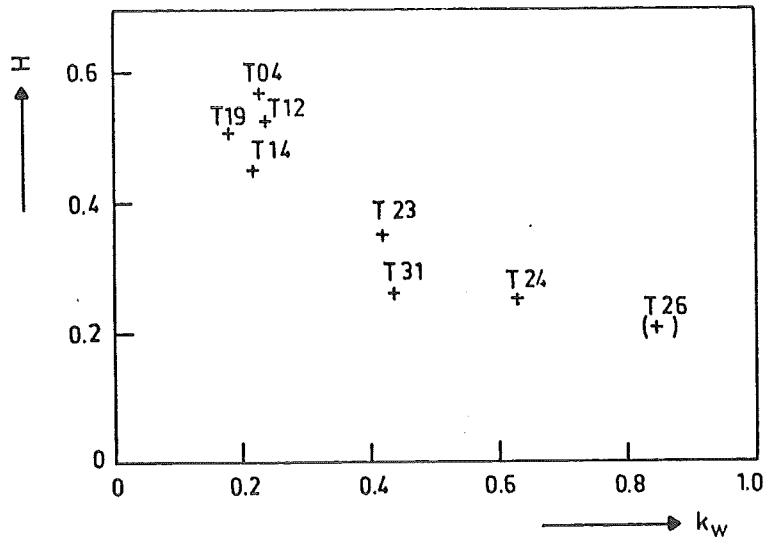

Figure 23. Measured height of alternate bars as a function of the transverse wave-number.

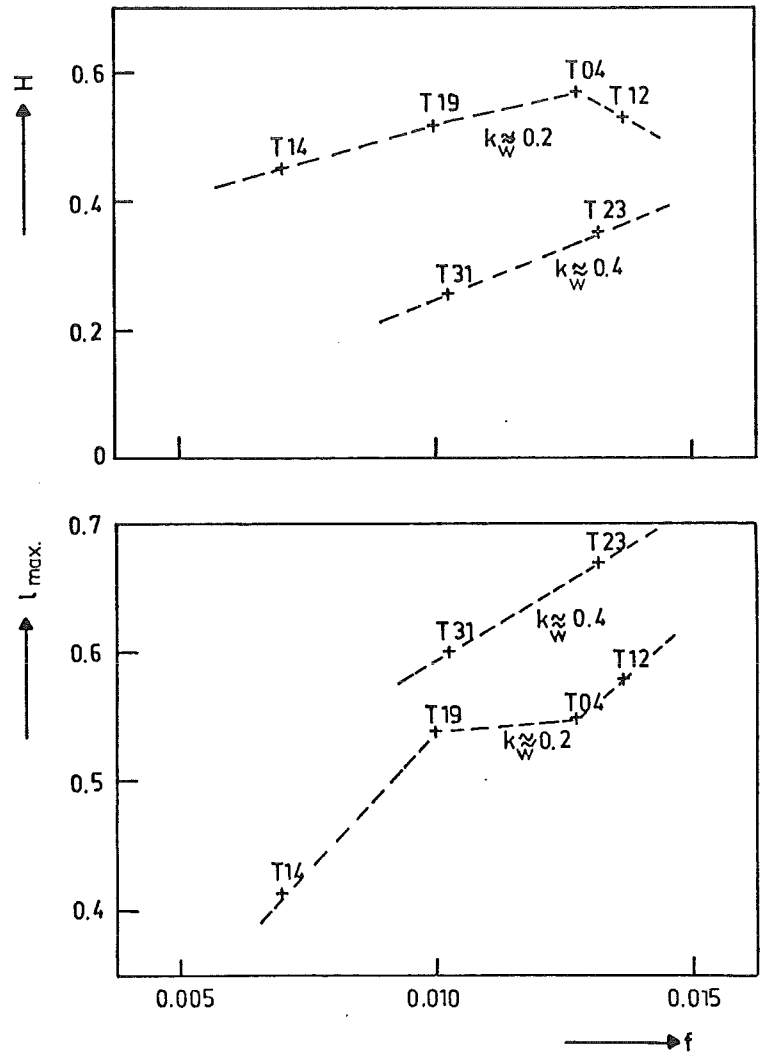

Figure 24. Measured height and length of alternate bars as a function of the roughness coefficient.